Calibration of HBV hydrological models using PEST parameter estimation

Deborah Lawrence
Ingjerd Haddeland
Elin Langsholt

1
2009

REPORT

Calibration of HBV hydrological models using PEST parameter estimation

Deborah Lawrence, Ingjerd Haddeland and Elin Langsholt

Norwegian Water Resources and Energy Directorate
2009

Report no. 1 - 2009

Calibration of HBV hydrological models using PEST parameter estimation

Published by: Norwegian Water Resources and Energy Directorate
Authors: Deborah Lawrence, Ingjerd Haddeland, Elin Langsholt

Printed by: Norwegian Water Resources and Energy Directorate

Cover photo: Near Sula gauging station, May, 2008. Photo by Ingjerd Haddeland

ISBN 978-82-410-0680-7

Key words: HBV hydrological model, automated calibration, PEST

Norwegian Water Resources and Energy Directorate
Middelthunsgate 29
Postboks 5091 Majorstua
0301 OSLO

Telefon: 22 95 95 95
Telefaks: 22 95 90 00
Internett: www.nve.no

January 2009

Contents

Preface

HBV hydrological models are important tools applied in water management by NVE. They are used, for example, by the Flood Forecasting Service for streamflow forecasts, in several projects considering the hydrological impacts of projected climate change, in the generation of weekly energy prognoses, and in the quality control of observed stream flow data.

There has long been a pressing need for a thorough review and recalibration of the operational HBV models, due to changes in climate and in the station network. The project "Verktøyprosjektet", initiated by NVE's Energy and Market Department with the aim of improving emergency preparedness in the energy sector, has further strengthened this need for updating model selection and parameterisation. In 2007, interpolated real-time observations of precipitation and temperature became available on a regular basis in the early morning, a product that made it possible to automate pre-processing of long timeseries of input data for the HBV model. Combining pre-processing with an automatic parameter estimation procedure (PEST), an automated procedure for calibration of a selection of catchment HBV models has been developed. This calibration tool represents a major improvement for maintenance and monitoring of the NVE flood forecasting model system and will also contribute to a more effective use of HBV modelling in climate change impact studies, as well as in other activities. The preparation of this report has been partially supported by funding from the Climate and Energy Systems project (funded by Nordic Energy Research, the Nordic energy sector and national institutions of the participating countries), the CELECT project (funded under the NORKLIMA programme of the Research Council of Norway) and the EU FP6 WATCH (Water and Global Change) project.

Oslo, January 2009

Morten Johnsrud
Director, Hydrology Department

Hege Hisdal
Section Head,
Hydrological Modelling Section

Summary

HBV hydrological models have been calibrated for 117 unregulated catchments based on 1 x 1 km grid-based precipitation and temperature input data. Five best fit models were calibrated for each catchment based on observed streamflow using PEST parameter estimation routines. The Nash-Sutcliffe (N-S) criteria and the volumetric bias for a calibration period (1981-2000 for most catchments) were used as objective functions for model optimisation. A final model was selected for each catchment based on N-S values and the volumetric bias for validation periods (1961-1980, 2001-2006; or as feasible for a given catchment), together with a qualitative assessment of the seasonal distribution of runoff and snow storage and the fit of the cumulative distribution functions for all flows, for peak flows and for low flows. Fifteen HBV parameters were calibrated during model optimisation for each catchment. The parameter estimation routines were effective in identifying best fit parameter sets based on multiple sets of starting values tested for model performance prior to optimisation. Model fits with N-S values > 0.70 for daily runoff were obtained in 90 catchments and for weekly runoff in 113 catchments. The model volumetric bias is < ±5% in 105 catchments and < ±2% in 56 catchments.

The sensitivity of the HBV parameters is also assessed during model optimisation with PEST, and the precipitation (rainfall) correction factor, PKORR, was found to be the most sensitive parameter in 100 catchments. In many cases, the sensitivity of this parameter is 1 to 2 orders of magnitude greater than other parameters. The precipitation (snowfall) correction factor, SKORR, was found to be the second most sensitive parameter in 87 catchments. The sensitivity of these two parameters underscores the importance of high quality precipitation input data for model performance. Model calibrations with poorer model fits are, in many cases, associated with smaller catchments in the western and southwestern regions of Norway. Comparisons with calibrations based on station data indicate that model fits are generally not improved when synoptic data are used, indicating that the weaker model performance in these regions do not arise from the use of grid-based, rather than station-based, input data. However, calibrated values for PKORR tend to be lower for catchments in western and southwestern Norway and are often below the lower bound previously used for this parameter (0.80), indicating that input precipitation values are often too high.

Simulation results from the HBV model runs for 115 catchments for the period 1961-2006 are available on the HYDRA-II system at NVE. The newly calibrated HBV models will be implemented in an upgraded flood forecasting system and integrated into new tools used for energy prognoses based on reservoir inflows, currently under development. They will also be applied in the assessment of the impact of climate change on hydropower supply within the Climate and Energy Systems project (funded by Nordic Energy Research, the Nordic energy sector and national institutions of the participating countries) and the CELECT project (funded under the NORKLIMA programme of the Research Council of Norway), and the EU FP6 WATCH (Water and Global Change).

1 Introduction

Hydrological models, based on the calibration of HBV in selected catchments, are used operationally by NVE in flood forecasting and have been used for this purpose on a regular basis since 1989. After the devastating 1995 flood, funding was provided to improve the flood forecasting service, and the number of calibrated catchments was increased and an automatic system for running daily prognoses was established. In the recent years, prognoses for nearly 80 catchments have comprised the basis for daily nationwide streamflow forecasts. Operational model runs are carried out every morning, based on the current climate observations and weather forecast from the Meteorological Institute (met.no). Observed daily streamflow is then used to update the streamflow forecast in proportion to the deviation between the last observed and simulated streamflow. Weekly aggregates of daily climate forecasts and HBV streamflow and snow storage forecasts are also used operationally to estimate energy inflow to reservoirs for hydropower production. Simulated energy inflow is, in turn, used to update the Samkjøringsmodellen (Power Market Simulator) for simulating the hydropower system. Calibrated HBV models are also applied, together with downscaled climate scenario data, to assess anticipated impacts of climate change on runoff during the next 100 years (*e.g.* Beldring, *et al*. 2006). Outputs from these analyses are relevant to issues such as future hydropower production potential in the Nordic region, reservoir dam safety and flood risk management.

Traditionally, input data for the HBV models have come from dataseries from individual climate stations. The climate station network changes in time, however, a feature that complicates the use of such data in the calibration of HBV models. Establishing a sufficiently long and homogeneous input dataseries for both model calibration and validation has been a major task when a new model is required or when recalibration of an existing model is needed, *e.g.* due to the closing of a climate station.In conjunction with the recent development and publishing of the seNorge web page (www.senorge.no) by NVE and met.no, a daily production line for gridded fields of precipitation and temperature and other water balance data and estimates was established. During 2007, these grids were made available early in the morning, making them a very useful source of input data for the flood forecasting system. The available grids now provide historical climate data in a 1 x 1 km^2 format for the period 1961 until the present day (Mohr and Tveito, 2008).

The availability of distributed precipitation and temperature grids is a prerequisite for the automated calibration procedure presented in this report. The grids are based on all available data at a respective point in time, providing a quasi-homogeneous time series of distributed fields. Model calibration can now be undertaken using a common procedure for input data for all catchments, together with a parameter estimation algorithm, with minimal manual intervention required. Such an automatic calibration procedure represents a major improvement in the tools available for the management of the flood forecasting system, as well as in procedures used for developing energy prognoses.

Model calibration for individual catchments has traditionally been achieved using manual adjustment of key model parameters within established ranges to obtain a best fit between observed and simulated discharge series. This procedure is time-consuming, is dependent on the skill and experience of the modeller, and is therefore prone to inconsistency between modellers. An advantage of the manual procedure is that it allows first-hand knowledge of hydrological conditions within a particular catchment and modelling experience in reproducing those conditions to contribute directly within the calibration process. An alternative to manual calibration is the use of automated computational routines for parameter selection, which are more efficient and remove some of the potential subjectivity of manual calibration. Mathematical and computational techniques for automated parameter optimisation and selection have significantly improved in recent years, making the approach both more feasible and accessible. The parameter estimation routine PEST (Doherty, 2004) is such a tool and has been used for several years at NVE for calibration of groundwater models, in addition to the HBV model. In the new calibration of models presented here, PEST was used to refine a set of five or more best-fit models for each catchment following uniform random sampling to establish feasible initial parameter values. User knowledge and experience was applied *via* additional qualitative criteria for model performance in the selection of the final model for each catchment.

This report presents an overview of the new calibration of catchment-scale HBV hydrological models for 117 catchments based on gridded precipitation and temperature data as the input timeseries and HBV parameter optimisation using PEST. Acceptable model fits were achieved in 115 of these catchments, and these new models will be implemented in an upgraded flood forecasting system, integrated into new tools used for generating energy prognoses currently under development, and applied in catchment-scale analyses of future climate change impacts on streamflow.

2 Catchment selection

The catchments selected for modelling are illustrated in Figure 1, and the gauging station names and numbers, the catchment area and the years for which streamflow data are available are given in Appendix 1. The selection comprises catchments previously used for flood forecasting and energy inflow forecasts, as well as new catchments for these purposes. Two principal constraints determine whether a catchment can be used for HBV modelling: 1) availability of a daily discharge timeseries of sufficient length and quality for model calibration and validation; and 2) absence of any significant regulation of streamflow. The majority of catchments in Appendix 1 have daily discharge series extending from 1961, the first year for which gridded climatological data are available, and all have been subjected to controls on data quality. Those which do not have data covering the entire period 1961 – 2006 have dates indicated in bold. Several of the gauging stations are not under the ownership of NVE and there are some variations in data quality between stations. All of the selected catchments have either no or minimal regulation (Pettersson, 2004). In addition to these constraints, 84 of these catchments were particularly chosen for their representativeness for energy inflow prognoses. Further details of that selection process are given in Holmqvist and Engen (2008), and the 84 catchments are identified as such in Appendix 1. Additional catchments were also added to the range of models used in flood forecasting to provide better spatial coverage and to include nested models representing different catchment scales where sufficient data are available to achieve this.

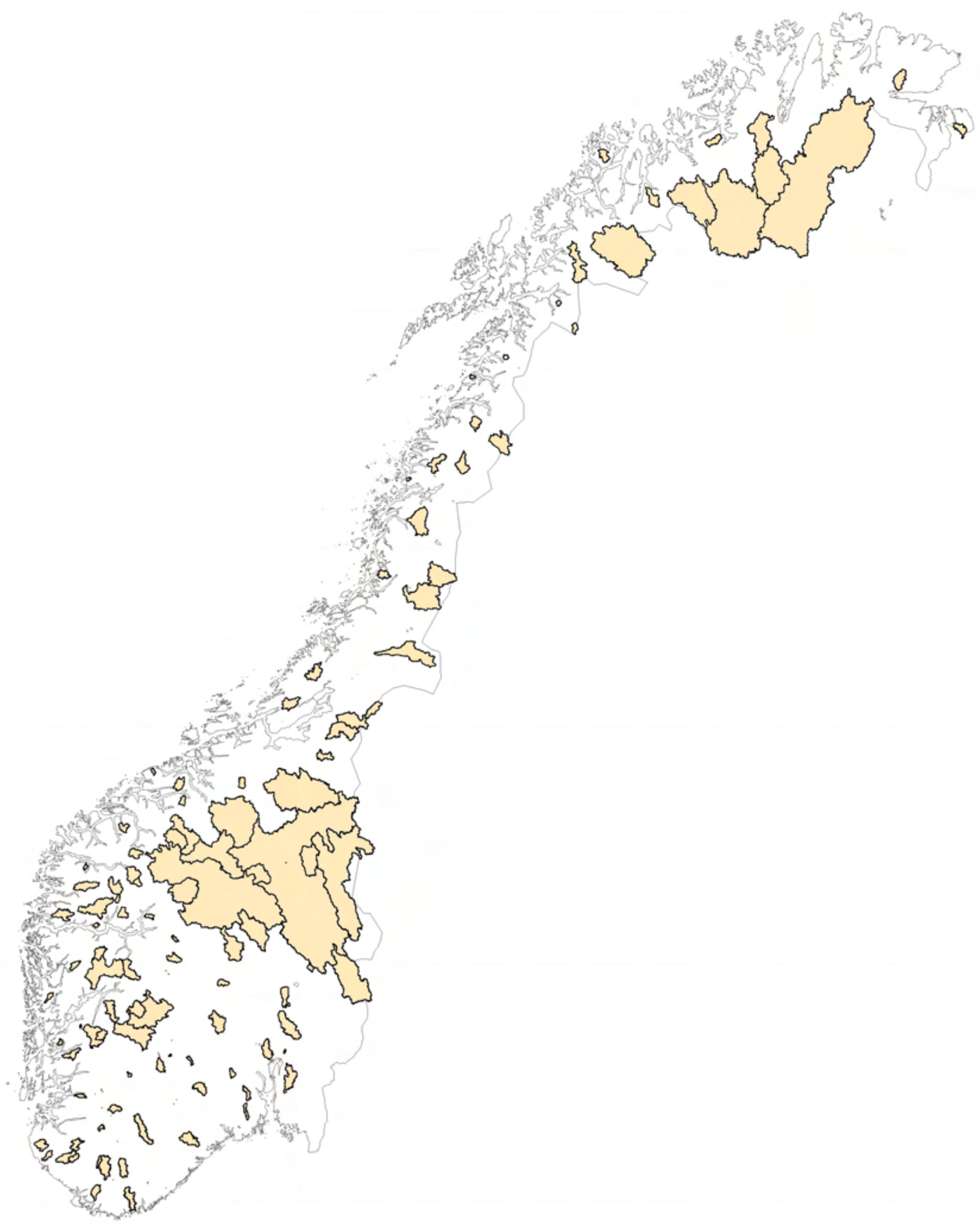

Figure 1. Location of catchments used in the PEST calibration of HBV models

3 The HBV model

The hydrological models calibrated for each catchment are based on the HBV precipitation-runoff model, which has been extensively applied in the Nordic region since its development in the 1970s (Bergström, 1976). The original model has undergone numerous revisions and improvements, and today there are several implementations of HBV available. In the applications reported here, the "Nordic" HBV model (Killingveit and Sælthun, 1995; Sælthun, 1996) was used. This version represents a 'lumped' catchment model in which the spatial structure of the catchment is not explicitly modelled. Ten equal area height zones from the hypsometric curve for the catchments are, however, used in the model snow routine, and land cover data is distributed by height zone. All processes, nevertheless, contribute directly to runoff at the outlet without internal routing between elevation zones. A more recent version of HBV performs calculations on a gridded basis throughout the catchment (Beldring, *et. al*. 2003), but also does not currently include internal routing between grid points. The gridded version was not used for model calibration, as it offers no significant advantages when simulating streamflow at the catchment outlet (contrasting with, for example, the simulation of snow cover, soil moisture or other distributed variables). Additionally, the model is more computationally intensive than the catchment version, making operational model runs, and not least post processing operations such as error estimation, more time consuming. The parameter optimisation routines used here are computationally intensive, as well, making it unfeasible to systematically apply them with the gridded model at this point in time.

Precipitation-runoff models such as HBV have been developed for forecasting purposes, where requirements demand relatively simple model structures that can be operationalised from readily available input data . The main structure of the HBV model is comprised of four storage components: snow, soil moisture, an upper runoff zone, and a lower runoff zone (Figure 2) and is discussed in detail in previous reports.

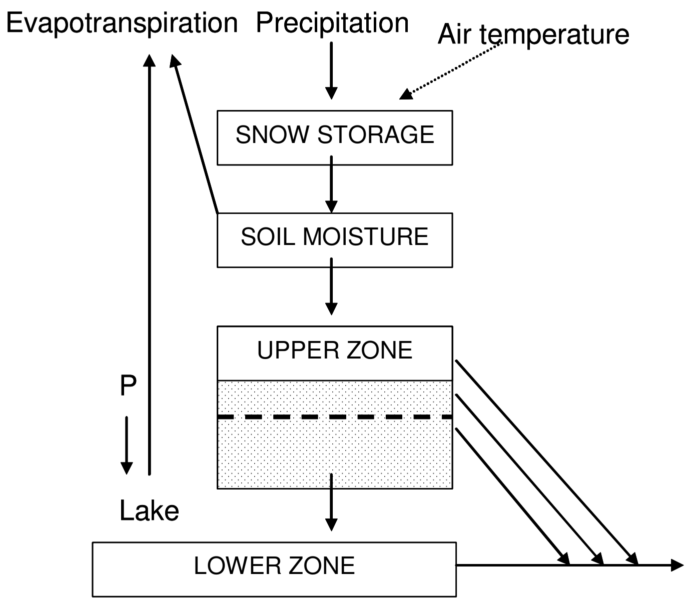

Figure 2. Storage components and principal fluxes in the HBV model

The processes within and fluxes between each of the four zones are governed by simplified expressions for the underlying physical processes (see Killingveit and Sælthun, 1995 for details). Processes are represented as linear or simple non-linear relationships, and all are controlled by parameters selected during calibration. The model is driven by timeseries (usually daily) of air temperature and precipitation, and model parameters are adjusted to achieve a best fit relative to streamflow observed at the catchment outlet. In the applications reported here, evapotranspiration is estimated by HBV using the temperature index method, rather than using monthly values as model input. The physical description of the catchment within the HBV model is based on the catchment area, the hypsographic curve for the catchment (area-elevation relationship), and the catchment land cover types. The climate input and catchment properties data are discussed in more detail in later sections of this report.

4 The optimisation procedure

4.1 PEST parameter estimation

Calibration of precipitation-runoff models, such as HBV, has been traditionally performed manually using a trial and error adjustment of model parameters to achieve an acceptable fit between modelled and observed timeseries. This procedure can be automated using Monte-Carlo techniques to sample the parameter space, seeking a best fit model parameter set by testing the performance of randomly-selected parameter combinations. Monte-Carlo random sampling is time and resource consuming, particularly when calibrating several parameters, as the number of trials required to ensure a full sampling of the parameter space grows exponentially with *n*, the number of calibration parameters (Solomatine, 1999; Bates and Campbell, 2001). Markov Chain Monte Carlo (MCMC) techniques have the advantage of being more 'intelligent' than direct uniform random sampling in exploring the parameter space, but their sensitivity to initialisation can lead to non-convergence (Haario, *et al*., 2006), making them difficult to apply in the systematic manner required for this work. New techniques for overcoming problems with MCMC methods (*e.g*. Smith and Marshall, 2008) often yield procedures which require even more computational time than uniform random Monte-Carlo sampling.

In the model calibrations presented here, PEST parameter estimation routines (Doherty, 2004) based on PEST *v*. 11.2 were used to calibrate values for HBV model parameters for each catchment. PEST is a parameter estimation program which uses a Gauss-Marquardt-Levenberg (GML) algorithm (Marquardt, 1963) to refine the iterative process underlying best-fit parameter selection. The algorithm combines advantages of the Gauss-Newton method and the steep descent method, producing a faster and more efficient convergence to an optimum. Following the use of initial parameter values in a trial model run, PEST applies a Taylor series expansion to express the relationship between the model parameters and the simulated (in this case, streamflow) values as a linear function. This linear function is then used to estimate new parameters, which are further tested by comparing newly simulated values with expected values. By comparing the relative improvements in successive runs, the degree of convergence (or non-convergence) can be evaluated and used to determine the subsequent direction of the optimisation. The principal advantages of the PEST algorithm are that it is based on a relatively robust optimisation algorithm and is more efficient than random selection of parameters by Monte Carlo methods. In addition, the routines and documentation are freely available and have been widely applied in the hydrological sciences (*e.g*. Liu *et al*, 2005; Lin and Radcliffe, 2005).

4.2 Comparison with SCEM-UA global optimisation

A disadvantage of PEST is that it uses a local optimisation routine, such that the final values obtained may be dependent upon the initial parameter values used in the optimisation. In other words, the optimisation scheme may become 'stuck' at local optima and fail to achieve a globally optimal parameter set (Duan, *et al*., 1993). Gradient-based methods, such as the GML algorithm in PEST, are particularly prone to this weakness (Gupta, *et al*., 2003). Stochastic global optimisation techniques have been developed as an alternative to local schemes; however, the model run times associated with these schemes increases significantly with the number of model parameters and can render them unfeasible for practical applications (Skahill and Doherty, 2006). In particular, local schemes, such as those used in PEST, can be initiated from multiple starting values within the parameter space to increase the likelihood that the full parameter space is sampled. This approach is simpler and often more efficient than global schemes. Before PEST was selected for use with HBV, calibration results derived from PEST were compared with results obtained using SCEM-UA (Shuffled Complex Evolution Metropolis algorithm), a global optimisation scheme which incorporates an adaptive MCMC algorithm (Vrugt *et al*., 2003). The comparison was based on 10 catchments, and the PEST calibrations were performed for 20 sets of initial parameter values. The average Nash-Sutcliffe criteria for the 10 catchments are illustrated in Figure 3. The results indicate that, in general, PEST achieved slightly better model fits during the calibration and validation periods than did SCEM-UA. It was, therefore, decided to use PEST for model calibration with multiple sets of initial parameter values for optimisation.

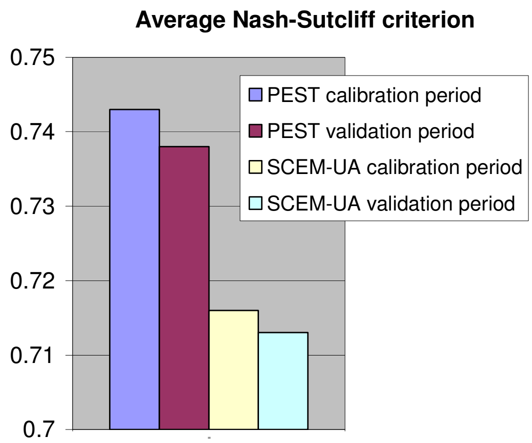

Figure 3. The average Nash-Sutcliffe score for the 10 test catchments

5 Input data

5.1 Grid-based precipitation and temperature data

A primary motivation for the automation of the HBV calibration procedure is the availability of 1 x 1 km gridded daily temperature and precipitation data from the Norwegian Meteorological Institute (met.no). These data are derived from the interpolation of daily observations of 24-hour mean temperature and 24-hour accumulated precipitation. For the purposes of HBV modelling, the gridded data provide a more systematic coverage in space and in time than one obtains from individual station data.

The daily temperature data are interpolated using the residual interpolation approach developed for monthly data and reported in Tveito, *et al*. (2000) in which the spatial distribution of temperature is modelled as comprising deterministic and stochastic components. The deterministic component is based on predictors established in previous work (Tveito and Førland, 1999) for describing large-scale spatial climate trends: the altitude of the grid cell, the mean and lowest altitudes within a circle of 20 km radius from the grid point, and the latitude and longitude of the grid point. Linear regression is used to model the deterministic component which is then removed from the data, and the residuals are modelled as a stochastic field using geostatistical techniques. The approach was developed for monthly data, but can also be applied to daily values (Tveito *et al*., 2005).

The procedure for precipitation is based on triangulation and entails creating a triangular irregular network (TIN) based on precipitation stations, which is then transformed to a regular precipitation grid. Gridded data are adjusted to give a vertical precipitation gradient of 10(%) per 100 (m) below an altitude of 1000 m and 5(%) per 100 m above an altitude of 1000 m in the final gridded data (Mohr and Tveito, 2008). The interpolated data provide a good representation of precipitation over large parts of Norway (Jansson *et al*., 2007). Problem areas include moutainous regions in southern area where there are long distances between stations. A comparison between extreme precipitation values derived from grid-based *vs*. station data indicates that grid-based methods give higher values for extreme events in Vestlandet than those derived from station data (Alfnes, 2007).

With the availability of gridded data, the HBV model can, in principle, be run with input precipitation and temperature values distributed by height zone. Alternatively, the HBV model internally adjusts P and T by height zone using calibrated precipitation and temperature lapse rates, such that a single daily value can be used as input. A comparison was made between calibration runs based on 1) spatially-averaged precipitation and temperature values; 2) precipitation and temperature values distributed by height zone; and 3) precipitation values distributed by height zone and temperature values spatially averaged for the catchment. The comparison was made for 70 test catchments. Results are illustrated in Figure 4 and indicate a very good correspondence between the N-S values obtained using spatially-averaged P and T values and P and T values distributed by height zone. The spatially-averaged values appear, in general, to perform slightly better than input data derived from distributed precipitation values and spatially-averaged temperature values. It was, therefore, decided to use the spatially-averaged values for model calibration.

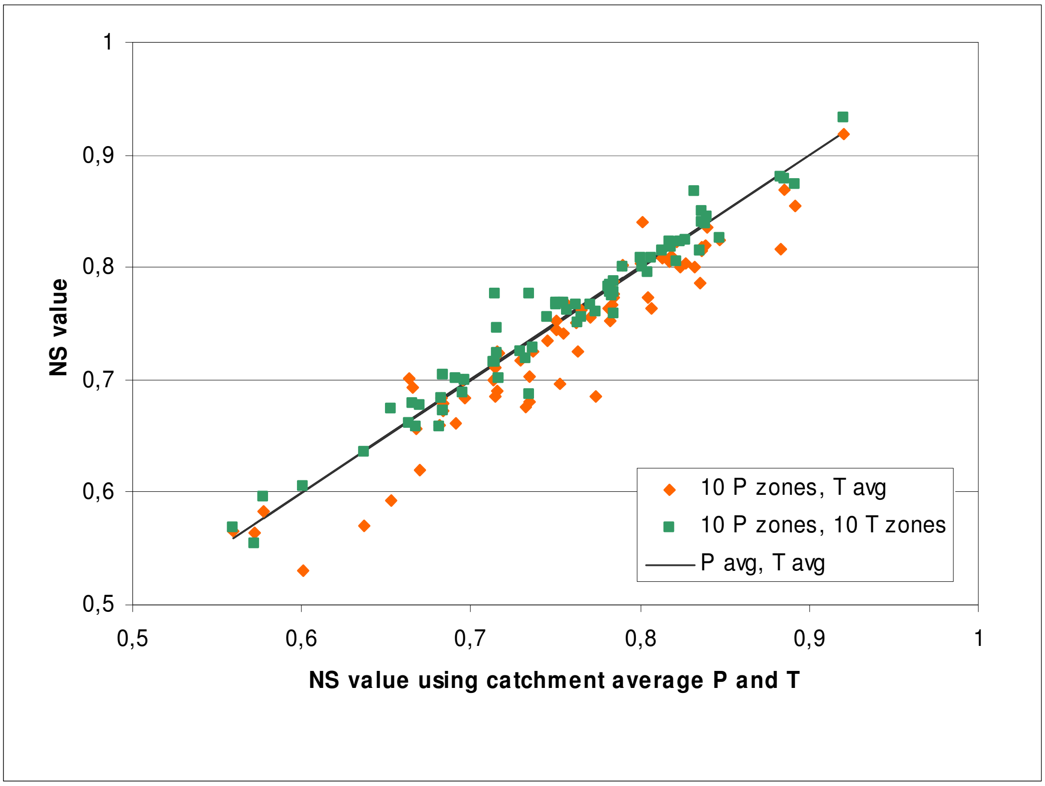

Figure 4: Optimal N-S values for 70 catchments using average precipitation (P avg) and temperature (T avg) values distributed by height zone as input to the HBV model, compared to N-S values using precipitation and temperature values distributed by height zone as input to the HBV model.

5.2 Catchment properties

Catchment properties required for the height-zone version of the HBV model include:

- Catchment area
- Upper and lower bounds on elevation for each of 10 equal-area height zones
- Elevation of precipitation and temperature stations
- Fractional lake area in each height zone
- Glacier-covered area as a fraction of total downstream catchment area for each height zone
- Dominant land cover type, secondary land cover type and fractional area of the secondary class in each height zone

These catchment properties were extracted using digital terrain model (DTM) and land cover raster files with a 25 m by 25 m cell size. The surface water catchment boundaries have been previously defined from the DTM for all active streamflow gauging stations in Norway by the VG (Water Resources – Geoinformation) section in NVE. Using those catchment boundaries, the hypsometric curve and associated equal area height zones were extracted for each catchment and the percentage of each land cover type within each height zone was estimated. Since grid-based rather than station-based precipitation and temperature are used in the calibrations, the elevation of the 'stations' was set to the median elevation value from the hypsometric curve for the catchment. In the case of catchments with transnational boundaries, land cover data were only available in the portion of the catchment located within Norway. It was therefore assumed that the spatial distribution of land cover, at least with respect to the dominant and secondary land cover types used in HBV, was similar on both sides of the national boundary.

Land cover types extracted for use with the HBV model are classified using the following categories: lake, forest, glacier, bog/marsh, agricultural/meadow, exposed bedrock and other. For each height zone, the fractional lake area, the dominant land cover type (forest, bog/marsh, agricultural/meadow or exposed bedrock) and the secondary land cover type as a fractional area are specified. Several HBV parameters controlling interception, snow distribution and snowmelt, soil moisture content and evapotranspiration vary with land cover type, and the values used for these parameters in model calibrations are given in sample vegtype.dat file in Appendix 2. The same vegtype.dat parameter values were used for all of the catchments.

6 Calibration procedure

6.1 Calibration and validation periods

Up to 45 years of data are available for model simulations in each catchment, as grid-based precipitation and temperature data are available from 01.09.1961. In approximately half of the catchments, observed discharge data required for model calibration also cover this entire period, and in many of the remaining catchments, discharge series begin in the mid-1960's to 1970's (Appendix 1). To ensure the use of a similar procedure in the majority of catchments, the period 1981 – 2000 was selected as a calibration period and the remaining data used for model validation. The first day of the model run was 01.09.first_year and the final day was 31.08.end_year, such that snow storage can be assumed to be zero at the beginning of the model run. In some cases it was necessary to adjust the years used for calibration and validation in individual catchments so as to avoid significant gaps or periods of questionable data quality in the observed discharge record. The calibration and validation periods used in each catchment are given in Appendix 3.

6.2 HBV calibration parameters and ranges

Fifteen HBV parameters were allowed to vary in the optimisation procedure during model calibration. These parameters are defined and the ranges for each parameter are given in Table 1. The parameter ranges are based on previous applications of HBV in NVE and largely follow the recommendations given in Sælthun (1996).

Table 1 – HBV parameter ranges used in PEST optimisation

HBV Parameter	***Description***	***Range considered***
BETA	Soil moisture parameter	1.0 – 4.0
CX	Degree day correction factor	1.0 – 5.0
FC	Field capacity – soil zone	50.0 – 500.0
KLZ	Recession constant – lower zone	0.001 – 0.1
KUZ1	Recession constant – upper zone 1	0.01 – 1.0
KUZ2	Recession constant – upper zone 2	0.1 – 1.0
PERC	Percolation – upper to lower zone	0.5 – 2.0
PGRD	Precipitation lapse rate	0.0 – 0.1
PKORR	Rainfall correction factor	0.8 (0.4) – 3.0
SKORR	Snowfall correction factor	1.0 (0.6) – 3.0
TS	Threshold temp. for snowmelt	– 1.0 – 2.0
TX	Threshold temp. for rain/snow	– 1.0 – 2.0
TTGD	Temp. lapse rate – Clear days	– 1.0 – – 0.5
TVGD	Temp. lapse rate during precip.	– 0.7 – – 0.3
UZ1	Threshold for quick runoff	10.0 – 100.0

In the cases of PKORR and SKORR, the standard lower bound on the parameter range (0.8 for PKORR and 1.0 for SKORR) was found to be too high for some catchments, and better calibrations in those catchments were obtained by reducing the lower bound on the parameter range to the lower value indicated in Table 1. Wider ranges for the parameters FC and KLZ were also used in an attempt to improve some model calibrations, but those changes generally had no effect on the final parameters selected during optimisation nor on the overall model fit.

6.3 Initial parameter values

PEST is, as discussed in Section 4, a local rather than a global optimisation routine. In order to increase the likelihood of finding the global optimal parameter set, PEST can be run with more than one set of initial parameter values. Accordingly, five or more initial parameter sets were chosen, one of which was the parameter set used in previous HBV simulations for the catchment, if available. For new catchments with no previous calibrated model, a parameter set chosen by the modeller was used for initial values. The remaining initial parameter sets for each catchment were selected randomly from the range for a given parameter:

Start_value = Lower_limit + Random_number * (Upper_limit - Lower_limit)

All of the initial parameter sets were tested in the HBV model and if the associated Nash-Sutcliffe value for the model fit was at least 0.25, the parameter set was optimised using the PEST routines. Initial parameter sets achieving N-S values lower than 0.25 were discarded and a new set was generated for testing. In a few catchments, the cut-off value of 0.25 was found to be too high, such that initial parameter sets could not be identified by this method. In those cases, the cut-off value was reduced until initial parameter values were successfully identified. In general, however, there was no relationship between the initial N-S values for parameter sets identified by random selection and the final calibrated N-S values for a particular catchment, following optimisation.

6.4 Calibration objective function

Optimisation of a parameter set is pursued with respect to an objective function, and in these calibrations the Nash-Sutcliffe (N-S) value for the calibration period (1981 – 2000, or as indicated in Appendix 3) was used for this purpose. The N-S value was based on the simulated versus the observed stream flow daily series together with the total accumulated difference between simulated and observed stream flow volume. Following optimisation based on the calibration period N-S value, each of the models was run for the validation periods (1961-1980 and 2001 – 2006, or as indicated in Appendix 3). The models were then ranked relative to their performance during the validation period, representing an independent test of the selected parameter set. Additionally, the volumetric bias for the validation period was used as a secondary measure of model performance for cases in which N-S values were equivalent for different parameter sets.

6.5 PEST optimisation settings

The PEST parameter optimisation algorithm can be refined for individual or subsets of parameters, and these specifications are given in the PEST control file. The PEST control file used in the calibrations is given in Appendix 4. In particular, parameter groups are used to define how difference increments used in the estimation of derivatives are calculated, the lower bounds on those increments, the type of differencing scheme that is applied and the method used for a particular differencing scheme. In this application, 9 parameter groups were defined to distinguish the lower bounds used for the difference increments. A forward difference scheme was applied for all parameters (variable ‘always_2’ in the control file). This scheme uses a parabolic forward differencing. The magnitude of difference increments was set to ‘relative’ for all parameters such that increments are calculated as a fraction of the current value of the parameter. Testing of the HBV model calibration routine with the central differencing scheme available for PEST was also undertaken. However, no significant improvement in the final calibration N-S values was achieved, although computational time was increased. Therefore, the simpler, parabolic forward-differencing scheme was used in the optimisations.

In addition to controls on the differencing scheme, the PEST control file can be used to specify parameter transformations, upper and lower bounds on the parameter range, limits on the maximum change of a parameter, and parameter scaling or offsets, if required. In this application, log-transformations were used for 7 of the parameters (Appendix 4). Two types of constraints can be placed on parameter change, factor-limited parameter change and relative-limited parameter change. These constraints are required to avoid overshooting the objective function optimum, and their respective suitability is dependent on the parameter range considered, especially the presence of a sign change or the inclusion of values greater than 1 (see Doherty, 2004, for further details). Accordingly, factor-limited parameter change was used for most of the parameters (Appendix 4), although relative-limited parameter change was required for two of the parameters (TX and TS).

7 Calibration results

7.1 Selection of best calibrated parameter set

The calibration procedure described in previous sections was applied to the 117 catchments illustrated in Figure 1, representing the gauging stations listed in Appendix 1. The procedure produced five or more best fit models for each catchment, often having very similar Nash-Sutcliffe values. In the selection of a final model for each catchment, the following criteria were considered

- N-S value for validation period
- Volumetric bias for validation period
- N-S values for the total simulation period, both daily and weekly
- Seasonal distribution of runoff by month
- Snow storage
- Cumulative distribution functions for all flow levels and for peak flow and low flows

To facilitate the selection, the results for the best five models for each catchment were imported into an EXCEL spreadsheet, such that some of these criteria could be assessed visually. Examples of the output from this program are given in Figures 5 through 10 below for Atnasjø (2.32). The models for each catchment were ranked for each of the criteria listed above by two individuals, Elin Langsholt and Ingjerd Haddeland, both with significant previous experience with model calibration and HBV model use in NVE. From this set of rankings for the models, a final best model was selected for use in the catchment.

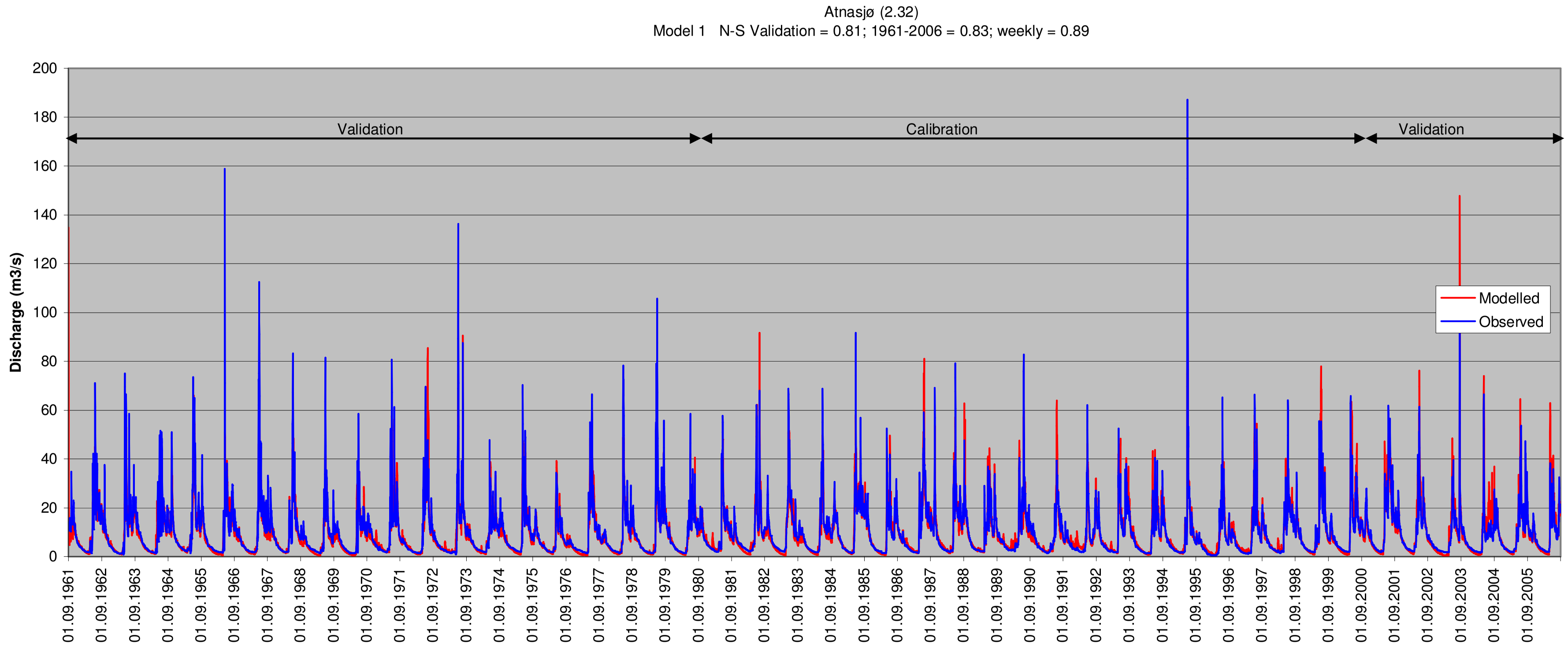

Figure 5. Modelled and observed discharge for the entire period 1961 – 2006 with calibration and validation periods indicated

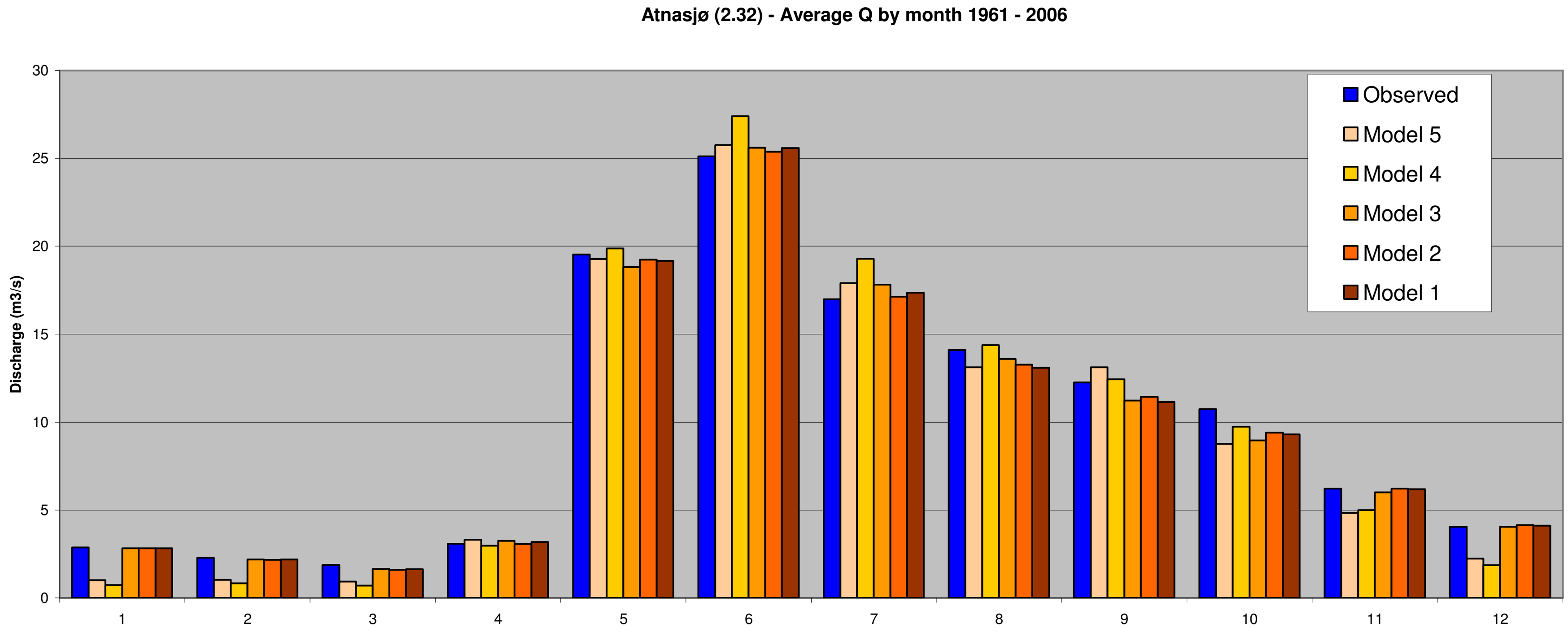

Figure 6. Average daily discharge by month for each model simulation and observed

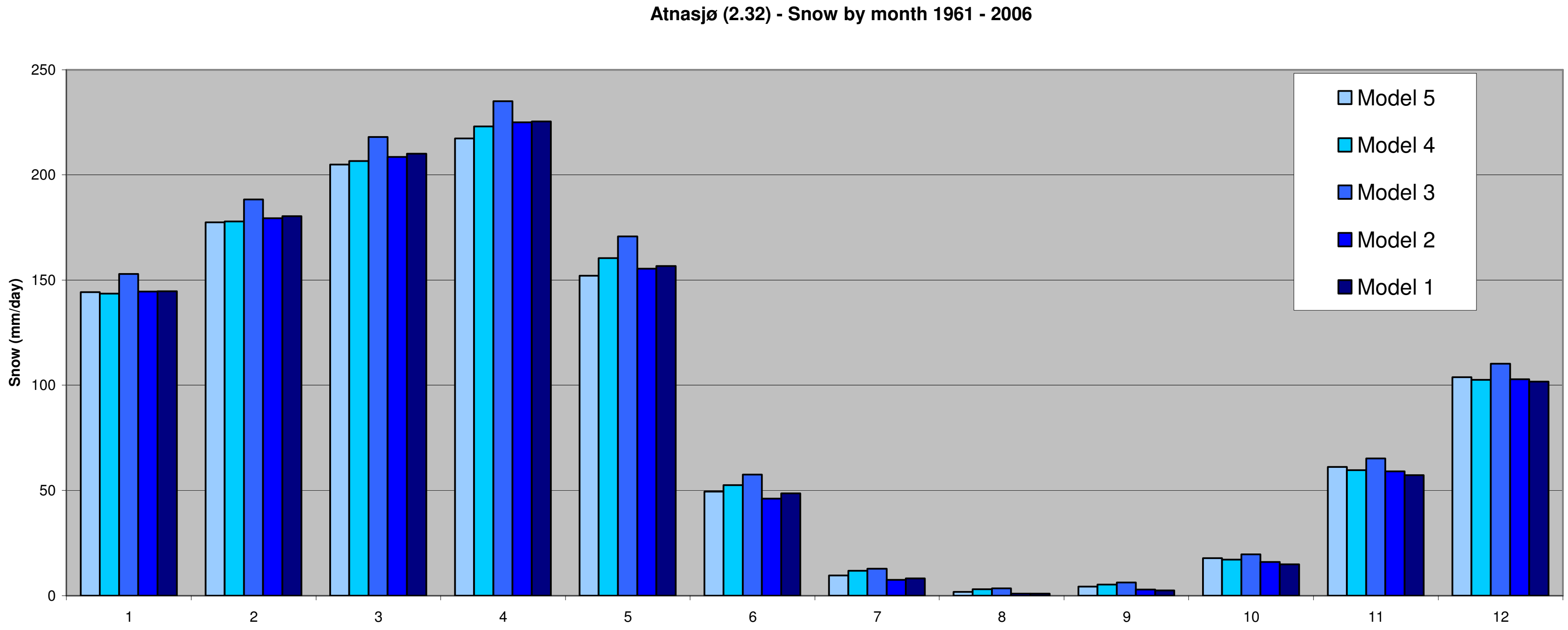

Figure 7. Snow storage by month for each model simulation

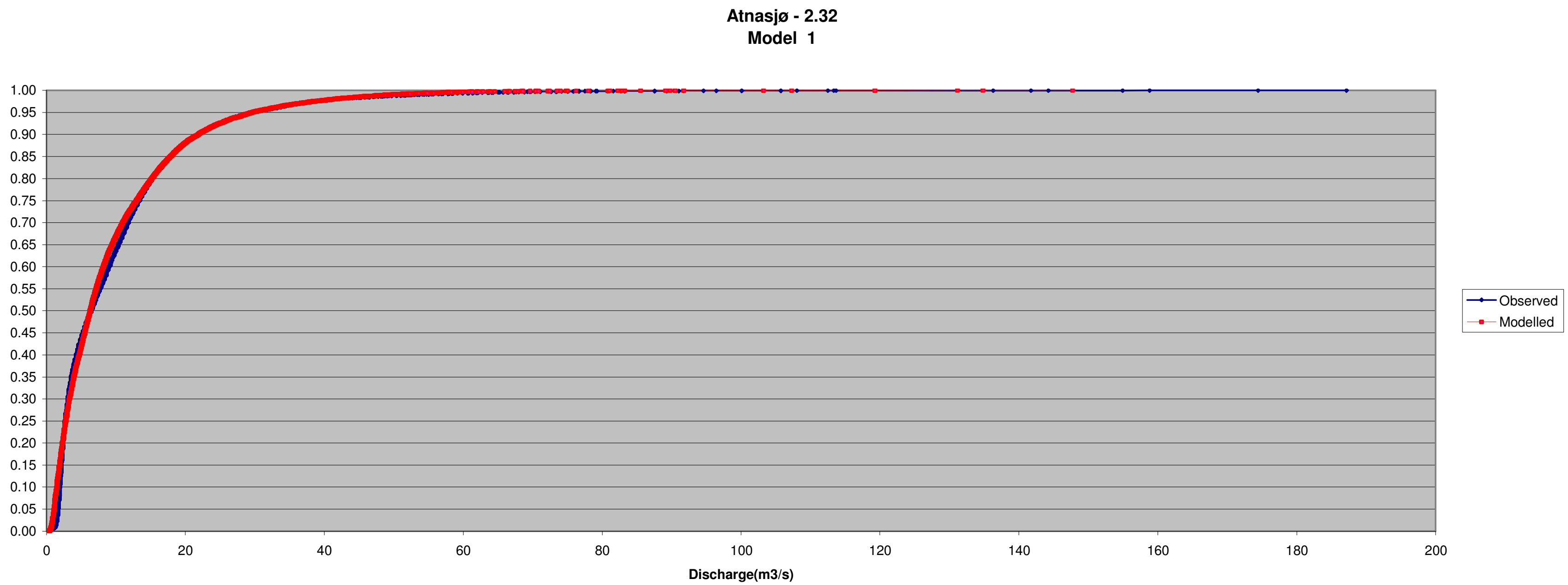

Figure 8. Observed and simulated cumulative distribution functions for non-exceedance flow levels

7.2 General performance

The daily Nash-Sutcliffe values for the selected models for the entire simulation period are illustrated in Figure 9 and are tabulated in Appendix 3. The daily values indicate overall good model performance in that 90 of the 117 catchments have values greater than 0.70. Excellent results with N-S daily values > 0.85 were achieved in 27 of these catchments. In general, larger catchments are associated with better model fits, as are catchments located in more easterly areas with relatively subdued topography. Poorer model fits tend to be associated with smaller catchments in areas with steep topographic gradients and high rainfall volumes.

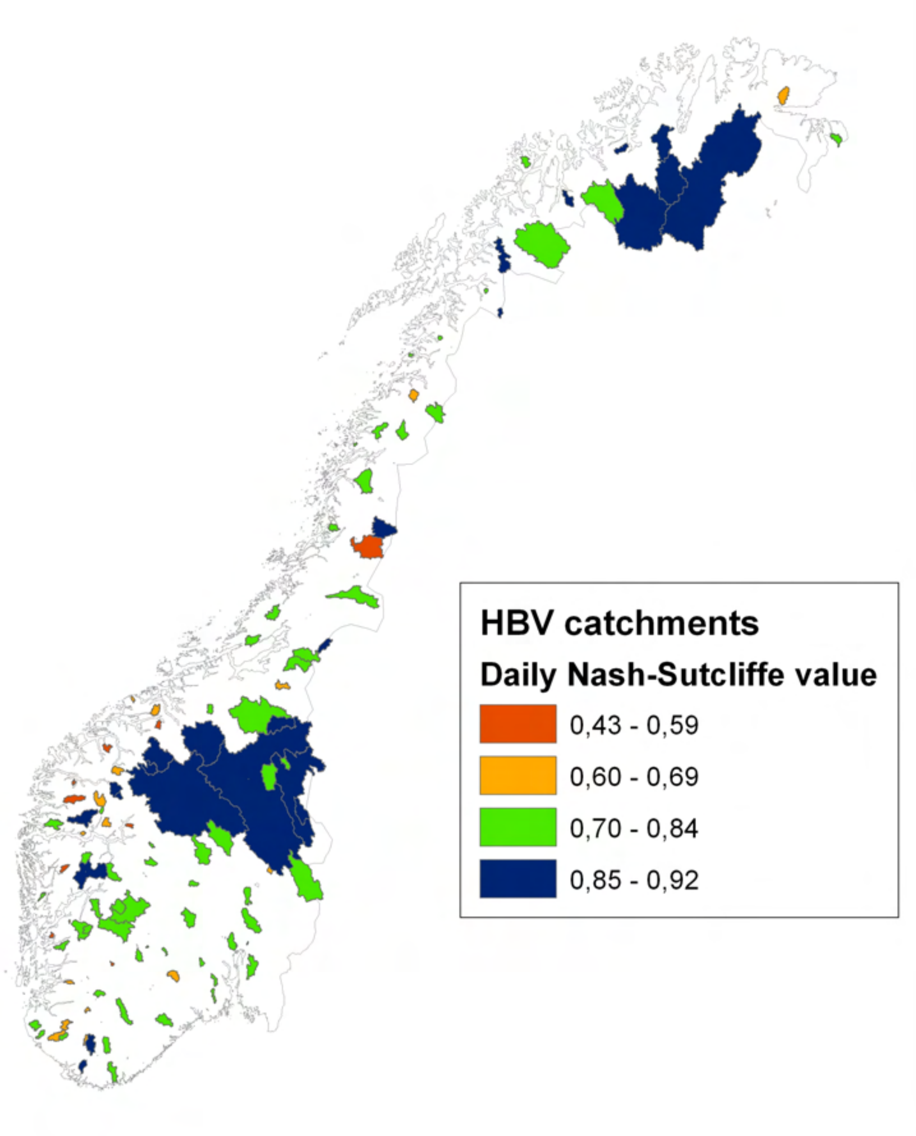

Figure 9. Nash-Sutcliffe values for each catchment model, calculated from daily observed vs. simulated discharge.

An estimation of weekly volumes is used for energy prognoses, and Figure 10 illustrates the Nash-Sutcliffe values for each catchment, calculated on a weekly basis. The weekly values suggest better model fits, with 112 of the catchments achieving N-S values > 0.70 and 47 having values > 0.85. The better model fits reflect the smoothing of peak flows that results when only weekly fluxes are considered. Again, some relatively weaker fits are seen in smaller catchments in the western region of Norway, but do also arise in three catchments in northern Norway.

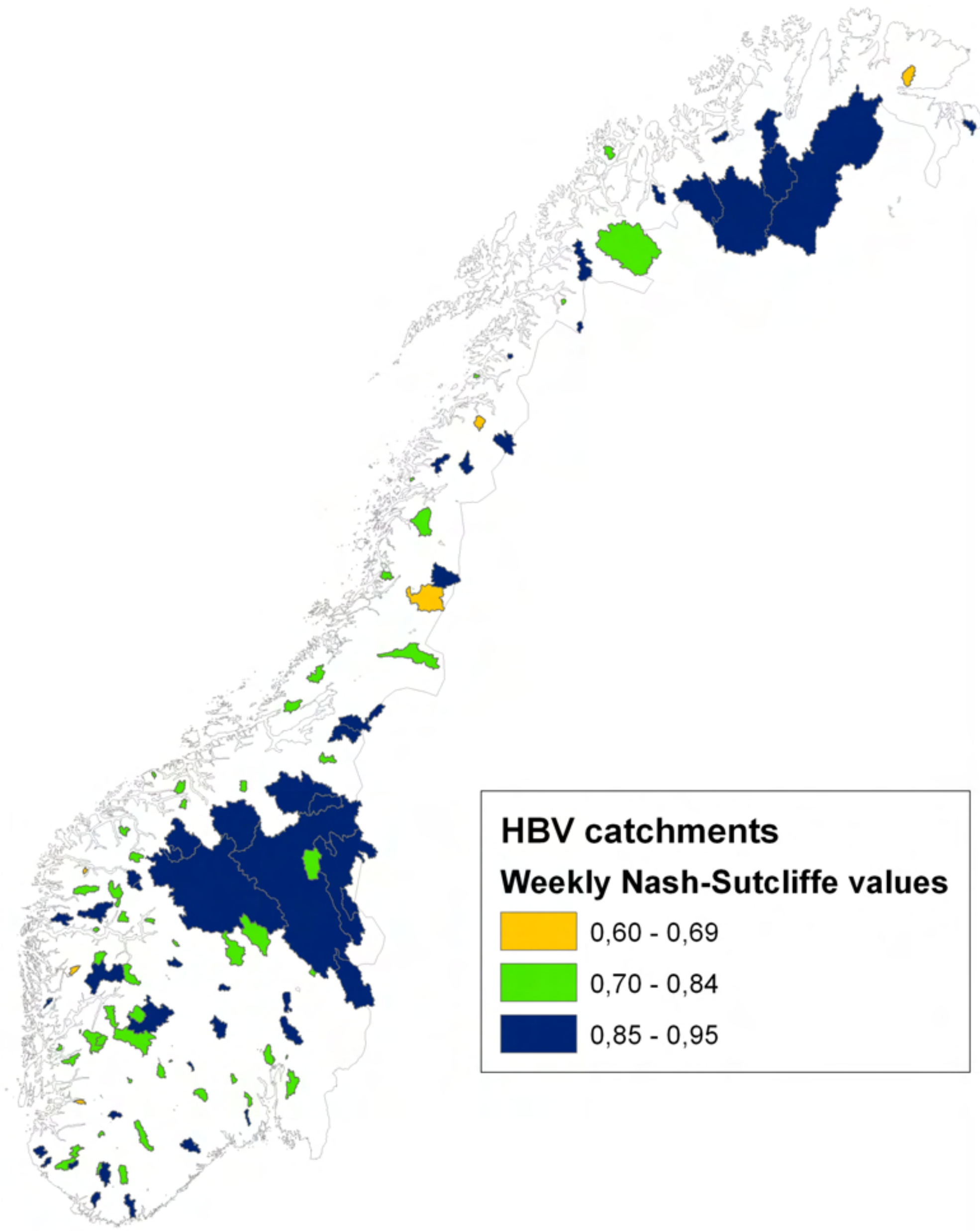

Figure 10. Nash-Sutcliffe values for each catchment model, calculated from weekly totals of observed vs. simulated discharge.

The volumetric bias was also calculated for each catchment based on the difference between the total observed and simulated runoff volumes, expressed as a fraction of the total observed runoff, and the results are illustrated in Figure 11 and tabulated in Appendix 3.

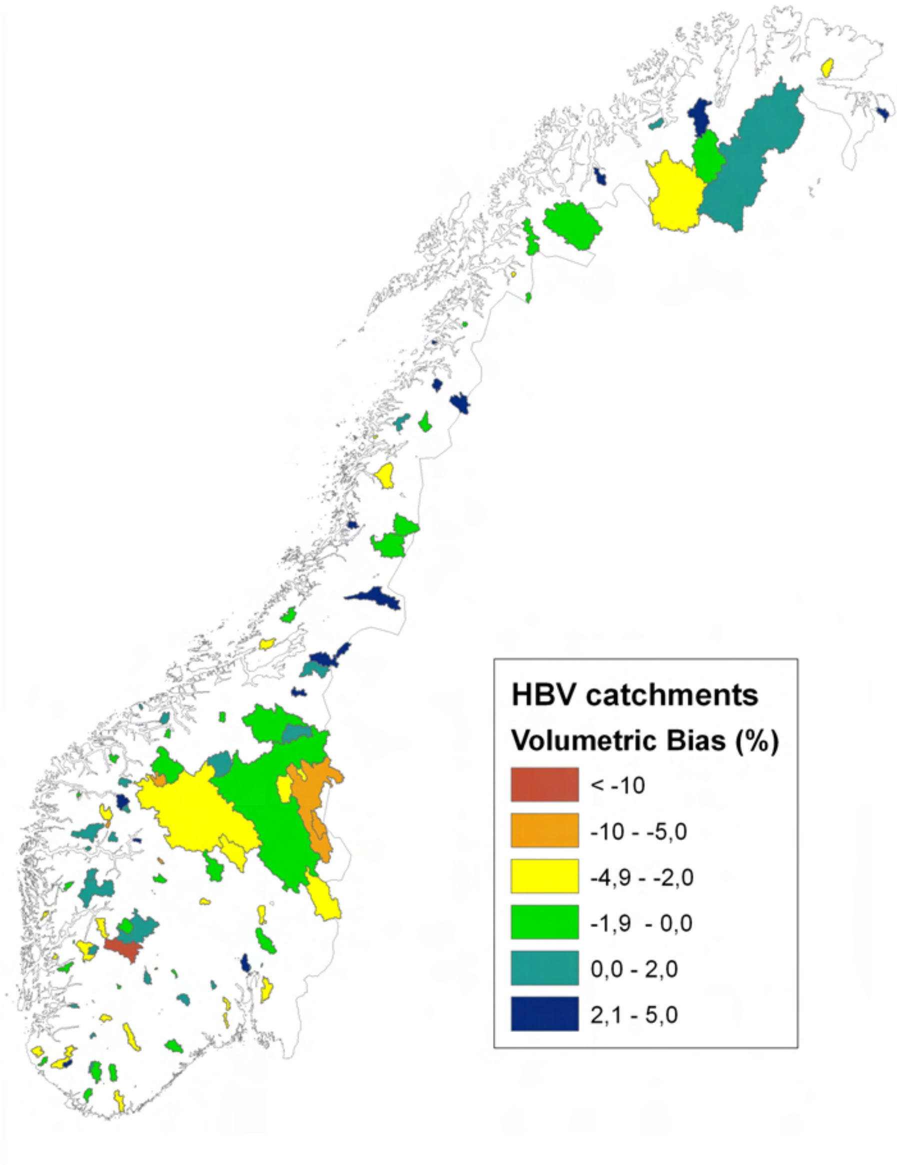

Figure 11. Volumetric bias (as a percentage of the observed runoff volume)for each catchment model

The majority of catchment models (105 of 117) have a volumetric bias less than ± 5 % and 56 catchments have models with a bias less than ± 2 %. Larger biases are, however, found in some catchments, and these tend to be negative, indicating an underestimation of the total runoff in those catchments.

7.3 HBV Parameter sensitivity and spatial distribution

PEST optimisation routines generate information about the relative sensitivity of calibrated parameters. The most sensitive HBV parameter identified in each of the catchments during calibration is illustrated in Figure 12 and indicates that the precipitation correction factor (PKORR) dominates the sensitivity in the majority of catchments (100 out of 117). In most cases, PKORR has a relative sensitivity which is one to two orders of magnitude greater than other parameters. In the remaining catchments, the lower zone recession coefficient (KLZ – 10 catchments), the precipitation lapse rate (PGRD – 6 catchments) or the degree day factor (CXF – 1 catchment) are the most sensitive parameter for the calibrated model.

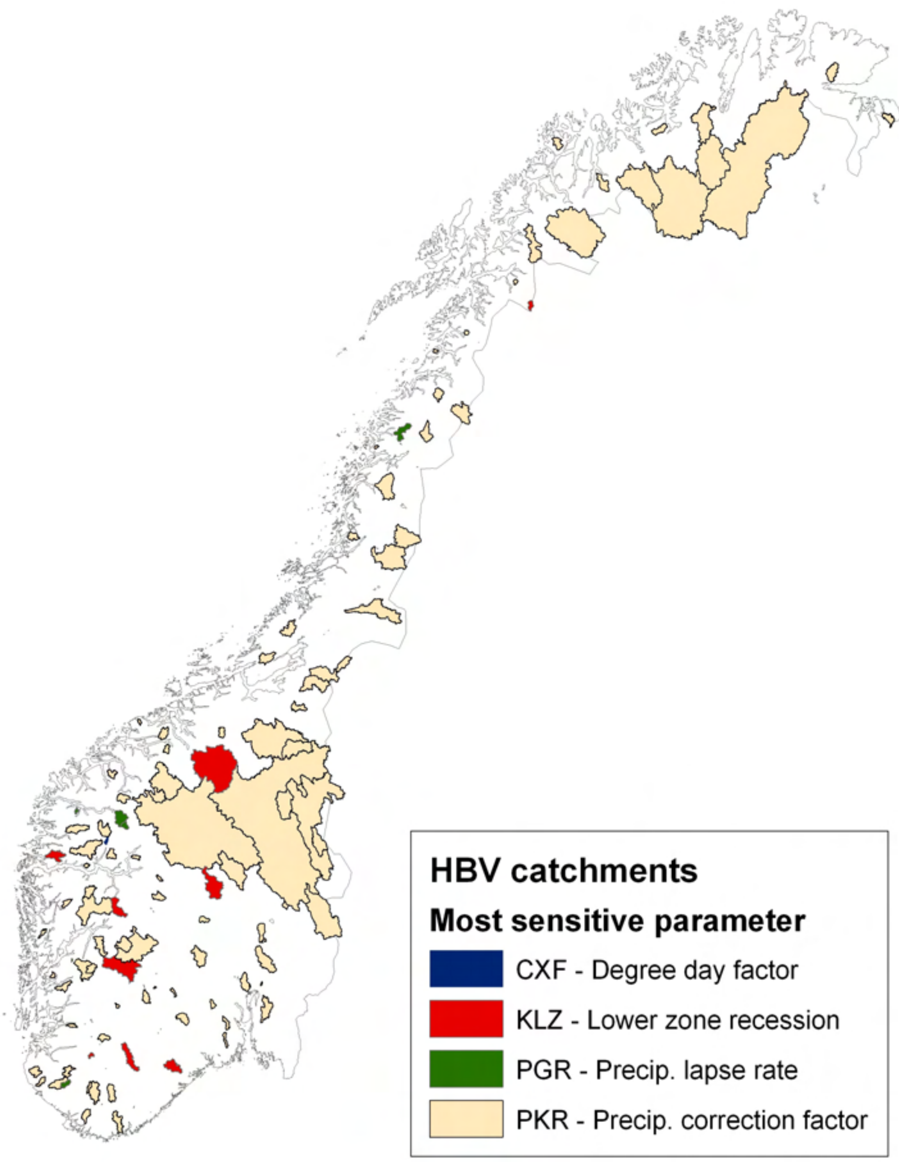

Figure 12. Most sensitive parameter in best model calibration for each catchment.

The catchments in which either PGRD or CXF dominate model sensitivity are all small catchments (area < 200 km^2) and six of the seven have a significant glacial cover in the upper height zones. In contrast, the catchments in which KLZ dominates the sensitivity tend to have catchment areas in the range of 200 – 2000 km^2 and have minimal or no glacial cover. However, in the vast majority of catchments, the precipitation correction factor dominates sensitivity. Additionally, the snowfall correction factor (SKORR) is the second most sensitive parameter in 84 of the 117 catchments. Taken together, the parameter sensitivities highlight the importance of high quality climate input data in reproducing observed streamflow.

The spatial distribution of the most sensitive model parameters was also considered and are illustrated for PKORR, SKORR and KLZ in Figures 13 – 15.

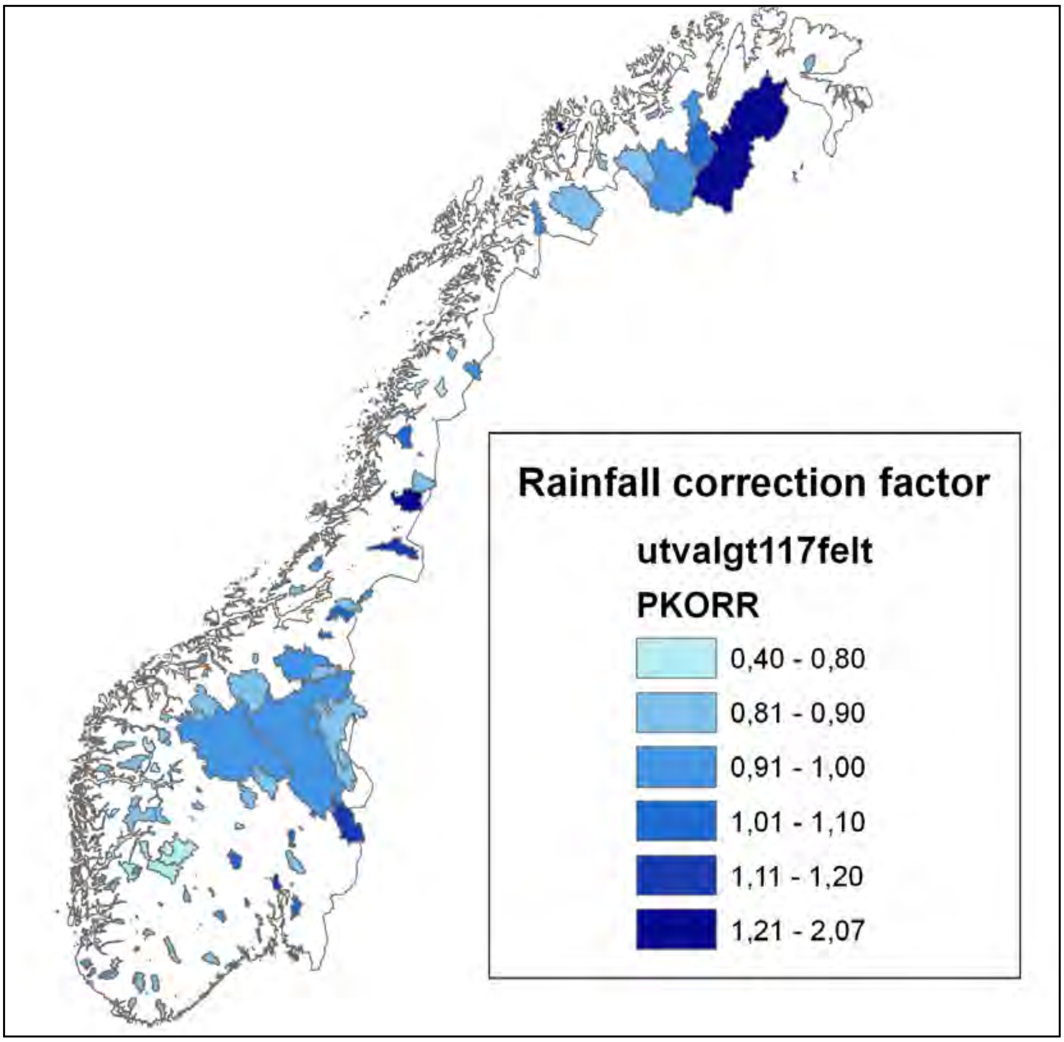

Figure 13. Distribution of calibrated values of the rainfall correction factor (PKORR)

Most of the catchments have calibrated values of PKORR which are less than one. A few smaller catchments in the mountainous region of south central Norway and in the western region of Norway have calibrated PKORR values between 0.40 and 0.80. This indicates that in these areas the input precipitation values, in this case derived from grid-based climate data, must be significantly reduced in order to achieve good model fits. Values close to one are generally seen in larger catchments, many of these catchments also have excellent HBV model fits (Figure 9). There are a few catchments for which the value of PKORR is greater than 1, and these tend to be located in more easterly locations.

The distribution of SKORR (Figure 14) shows a less consistent spatial pattern than does PKORR. However, in some cases, higher values of SKORR are associated with catchments having lower values of PKORR. This might be expected if SKORR functions to adjust the effects of a low precipitation correction factor in the water balance. This pattern, though, is not universally true, and there is no significant correlation between the calibrated values for these factors when all catchments are considered. In particular, several of the catchments in the southern and western regions which have low PKORR values also have values of SKORR less than one.

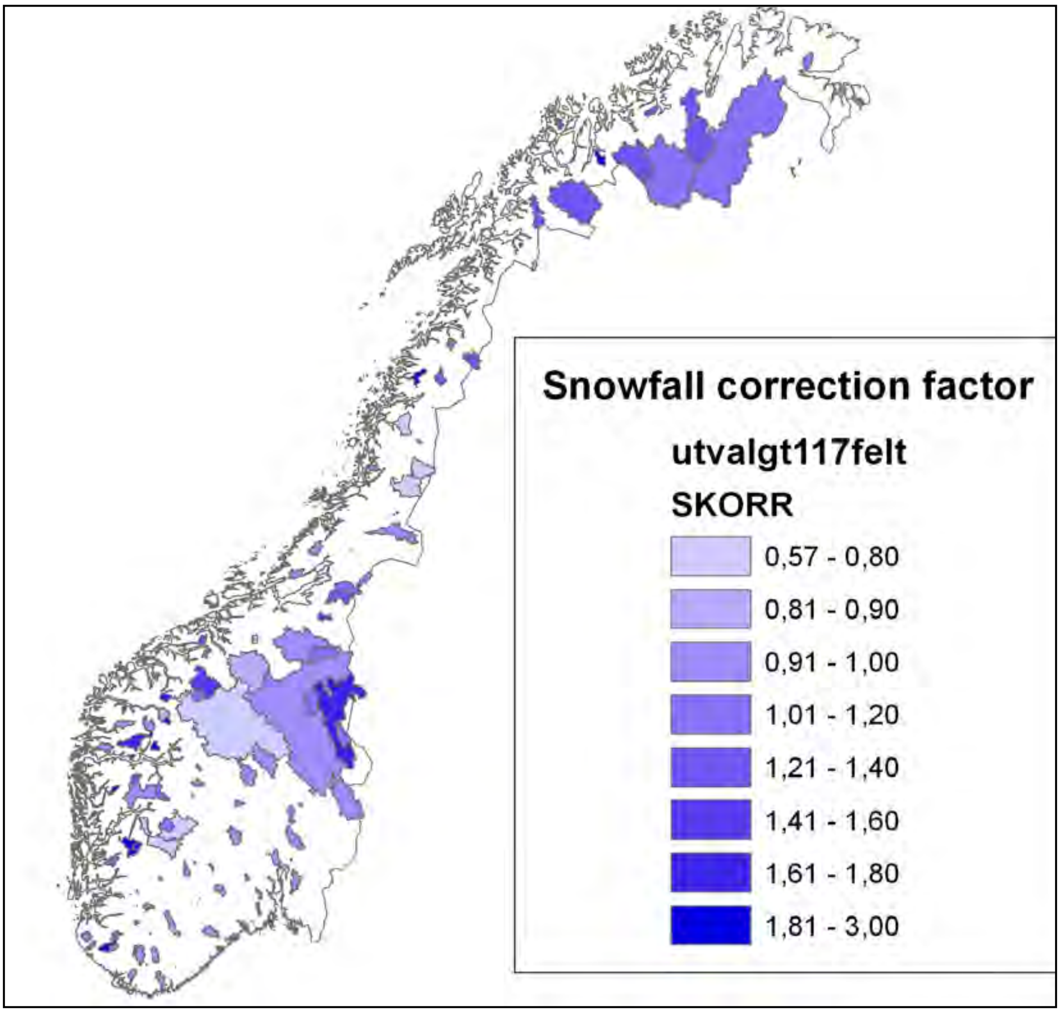

Figure 14. Distribution of calibrated values of the snowfall correction factor (SKORR)

The HBV hydrological model has simplified surface and subsurface flow pathways, controlled by calibrated recession constants, KZ1, KZ2 and KLZ. Of particular interest is KLZ, as it represents the slower subsurface flux of water within the HBV model, often conceptualised as corresponding to groundwater flow. The distribution of the KLZ parameter is illustrated in Figure 15 and indicates that best-fit parameters for KLZ cover the full range of available values from 0.001 (slowest flow) to 1.00 (fastest flow). There is a tendency for lower values of KLZ to be associated with the largest catchments in areas of more subdued topography. The highest values of KLZ are associated with smaller catchments, and many are located in the more mountainous areas, as might be expected due to the presumably faster and shorter flowpaths in those catchments.

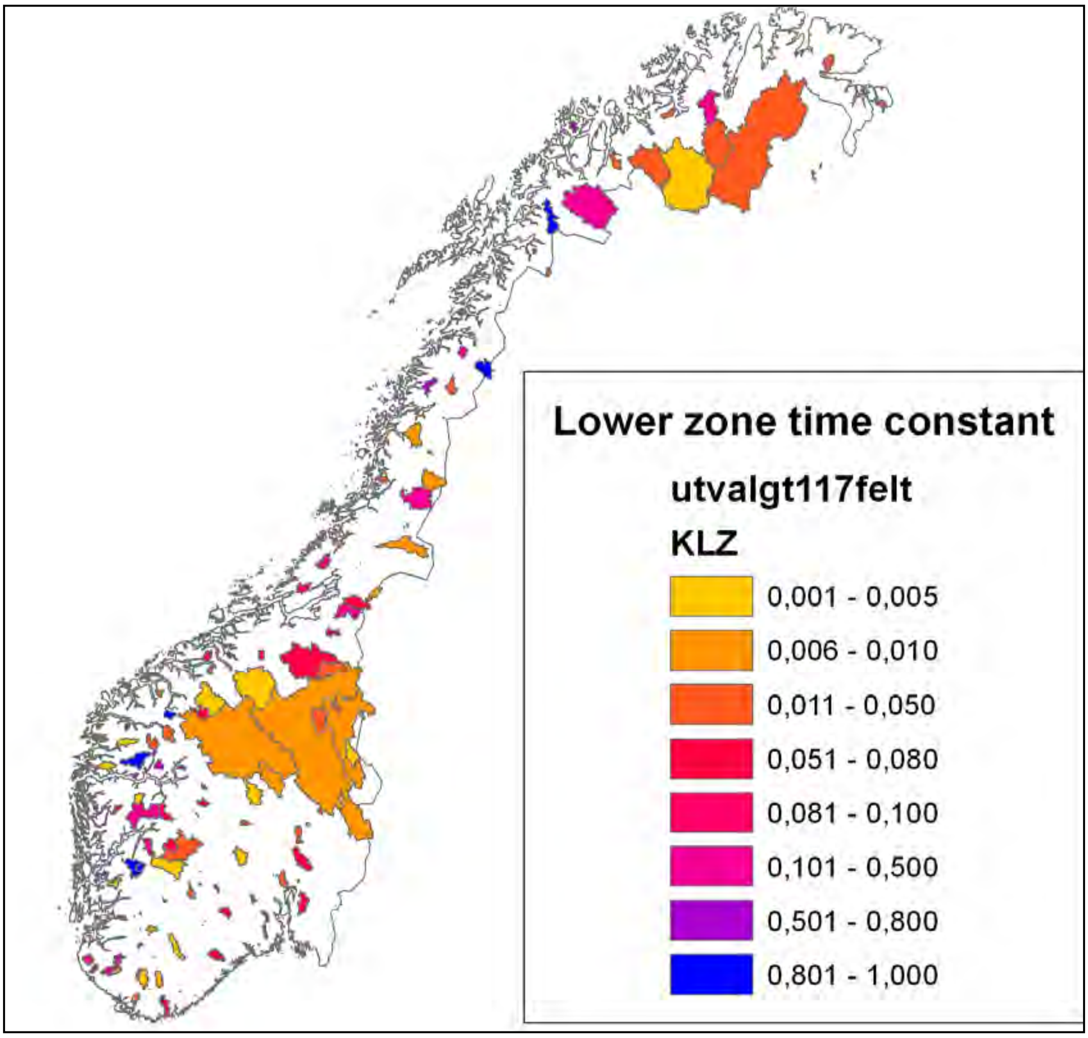

Figure 15. Distribution of calibrated values of the lower zone recession constant

7.4 Discussion

Although good calibrations were achieved for most of the catchments, there are a few problem areas. In particular, calibration for the following two catchments:

- Dyrdalsvatn (55.5) – Daily N-S = 0.53; Weekly N-S = 0.72
- Svartavatn (62.18) – Daily N-S = 0.51; Weekly N-S = 0.67

did not yield a suitable model, when evaluated with both quantitative (N-S values and volumetric bias) and qualitative (snow cover, seasonal runoff distribution, cumulative distribution functions) criteria. These models are, therefore, not included in the current set of operational models. Additionally, less than optimal model fits are found in the following catchments: Bjørnstad (139.15), Djupevad (42.2), Fetvatn (97.1), Hovefoss (84.11), Lislefjødd (21.47), Krokenelv (75.23), Vistdal (104.23), Skjerdalselv (86.12) and Sæternbekken (8.6). The majority of these catchments share some common features in that all, excepting Bjørnstad (139.15) and Hovefoss (84.11), have catchment areas less than 90 km^2 and most are characterised by steep catchments gradients. Additionally, 9 of the 11 catchments are located in the western and southwestern regions of Norway.

Motivated by the weaker model calibrations in areas associated with high precipitation volumes, a comparison was made between model calibrations based on grid-based precipitation and temperature data and data derived from synoptic weather observations. The calibration and validation periods were adjusted for each of 6 catchments to reflect periods for which synoptic data were available for local stations (Table 2).

Table 2 – Comparison of model calibrations with grid-based vs.synoptic input data

Discharge station	***Synoptic station***	***Calibration period***	***Validation period***	***N-S value: Grid-based***	***N-S value: Synoptic***
8.6 - Sæternbekken	Blindern	1976-1986	1987-1997	0.51	0.46
42.2 - Djupevad	47890 Opstveit 46910 Vats	1989-1994	1994-1999	0.41	0.40
55.5 - Dyrdalsvatn	50540 Bergen	1983-1994	1994-1999	0.43	0.42
75.23 - Krokenelv	54120 Lærdal	1999-2003	2003-2006	0.60	0.64
86.12 - Skjerdalselv	508070 Sandane	1982 -1994	1994-2006	0.54	0.59
139.15 - Bjørnstad	Fiplingvatn	1999-2003	2003-2006	0.67	0.57

Best-fit models were calibrated for each set of input data based on 10 initial parameter sets. The N-S values for the validation period are given in Table 2 and illustrate that in 4 of the 6 catchments, the N-S values are actually worse, rather than better, when one uses synoptic, rather than gridded data. However, two of the smallest catchments, Skjerdalselv (catchment area = 24 km^2) and Krokenelv (catchment area = 46 km^2) have slightly improved N-S values for the models derived from synoptic precipitation and temperature data. In general, however, the comparison does not indicate that grid-based precipitation and temperature data are responsible for the weaker model fits.

A weakness in the model results which applies to all catchments is that the simulations have a tendency to underestimate flood peaks. Figure 16 shows observed and simulated mean annual flood and the 5-year flood for most of the calibrated catchments and clearly indicates a systematic underestimation of peak flows for both flow indices. In operational flood forecasting, both the observed and simulated flood values are used, such that this systematic bias in the results is of particular relevance in that context and is discussed further in the final section of this report.

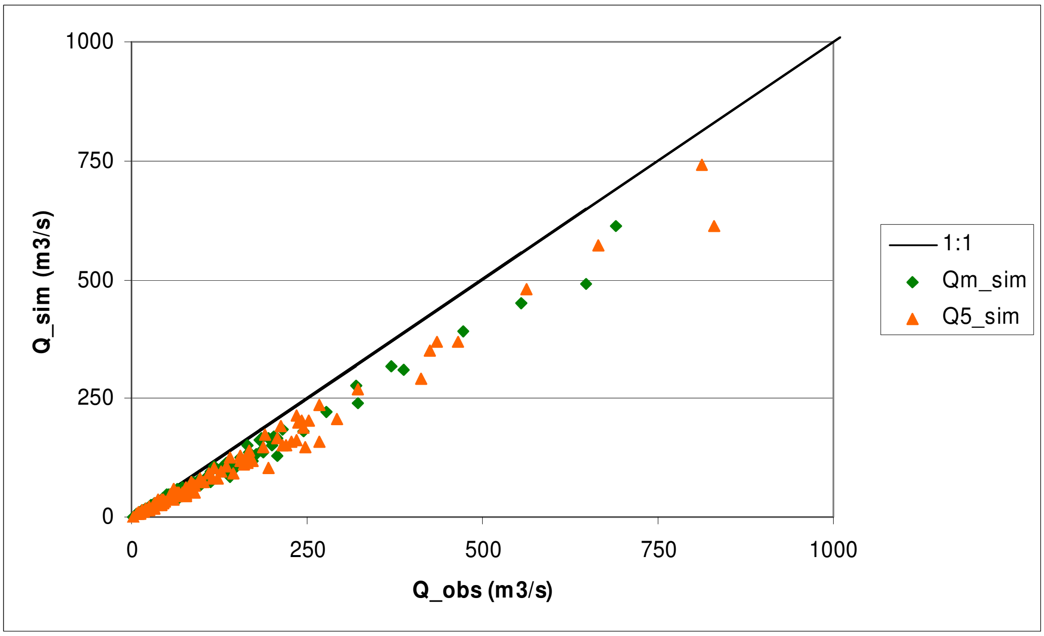

Figure 16: Observed (Q_obs) and simulated (Q_sim) mean annual (Qm) and 5-year (Q5) floods in the catchments having Q_sim and Q_obs less than 1000 m^3/s (112 out of the 115 catchments).

Estimation of reservoir inflow for energy prognoses are based on weekly, rather than daily model simulations, resulting in a smoothing of the effects of individual peak flows. The weekly N-S values for the calibrated models are > 0.70 in 112 of the catchments and > 0.85 in many of them, indicating very good model performance in most of the catchments. Additionally, the seasonal patterns of runoff and snow storage were considered qualitatively in the selection of the final models. The volumetric bias is also relevant for energy prognoses, as it indicates the extent to which total runoff volumes are either over- or underestimated by the models. Nine of the 84 models selected for future use in conjunction with energy prognoses have volumetric biases that are greater than ±5%: Tora 2.291 (-6.2%), Eggedal 12.178 (+6.87%), Groset 16.66 (-5.47%), Brekkebru

72.5 (+10.34%), Sula 73.27 (-6.89%), Bøyumselv 78.8 (-9.07%), Hovefoss 84.11 (-5.56%), Skogsfjordvatn 200.4 (+8.04%) and Engeren 311.640 (-6.80%), which are less than optimal and should be taken into account in the application of these models. In general, however, is expected that the increased number of catchments will give a better spatial representativity and thereby improved reservoir inflow estimates.

8 Suggestions for further developments

The automated application of PEST with grid-based input climate data for HBV model calibration makes feasible the generation of a large set of models in an effective and efficient manner, each model developed using a common procedure. Although model performance is not always improved in individual catchments over earlier calibrations, the system for calibration developed represents a major improvement with respect to maintenance and monitoring of the flood forecasting model system. The calibration tool makes it a simple matter to update recalibrations when input data, rating curves or other circumstances change. Moreover, it makes the system more flexible, in that new catchment models can be readily calibrated and included in the operational model set. Additional efforts in improving the calibration procedure should be given priority in the near future, to further optimise these achievements.

The model calibrations have highlighted several issues which warrant further investigation. Among these are the objective functions chosen for model calibration. In this application, the Nash-Sutcliffe criterion, based on the simulated versus the observed stream flow and the accumulated difference between simulated and observed stream flow volume was used as the objective function for the selection of initial parameter sets and for the PEST optimisations. Many models with very good N-S values, have volumetric biases in the range of ± 2 – 5 %. This bias could be reduced if model calibration were pursued using a larger weighting for the volumetric bias in the objective criterion. Better model fits could also be obtained for many of the factors that have here only been evaluated qualitatively (for example, the cumulative distribution functions), if these were explicitly evaluated during optimisation. In particular, the calibration of models used for flood forecasting purposes, could be undertaken with explicit reference to model performance at high flows, for example, the fit of the cumulative distribution function above the 95% or 99% non-exceedance level. Alternatively, within the PEST routines, the user has the option of weighting particular observations in the observed timeseries, such that flood events could be given more weighting than normal flows within the calibration process.

Poorer model fits are often associated with the western and southwestern regions of Norway where precipitation volumes are high. Additionally, the spatial distribution of the rainfall correction factor, PKORR, suggests that grid-based data particularly overestimate rainfall in this area. Further work is required to develop methodologies for acquiring representative precipitation data for model calibration. It is not likely that the density of precipitation gauges will increase in the future, but NVE and met.no currently collaborate on a research project (Bedre Romlige Estimater av Meteohydrologiske Synoptiske felt - BREMS), which aims to improve the spatial interpolation of precipitation and temperature from existing stations. It is anticipated that the results of this research project will be beneficial in future recalibrations of the HBV model catchments.In addition to weaknesses associated with input data, some of the smaller catchments have poorer model fits, possibly due to a mismatch between the HBV model time step and the runoff response in these catchments. The current HBV model operates on a daily step, and in smaller catchments, a higher degree of temporal resolution may be required in order to capture the processes contributing to runoff, particularly peak flows during extreme rainfall events. However, such modifications are also dependent on the availability of input and observational data at, for example, an hourly resolution for model testing and development.

Snow storage volume and seasonal distribution has only been considered qualitatively in the selection of the calibrated models, based on figures for each catchment such as illustrated in Figure 7. In some catchments, there is the potential to calibrate models with respect to satellite observations of snow coverage (SCA), in addition to observed streamflow. Previous studies have shown that using satellite observed SCA in the calibration of HBV models may be useful, especially in years with unusual weather conditions. (*e.g.* Alfnes *et al.* 2005). The effect of calibrating other state and flux variables, such as soil moisture content or groundwater levels, as available, remains to be pursued. Such an approach could provide better constraints on the parameter space, making the calibrated catchment parameter sets more regionally consistent, which is a prerequisite for applying HBV-type models for predictions in ungauged catchments. In general, a focus on additional state variables will tend to improve the representativity of a model's water balance elements, an important feature in the estimation of energy system inflow (Colleuille *et al*. 2008).

Finally, the PEST calibration procedure generated information on the sensitivity of the HBV models parameters used in the optimisation. The relative sensitivity of these parameters indicate that only four dominate the performance of the models calibrated here: PKORR (precipitation correction factor), SKORR (snowfall correction factor), PGRD (precipitation lapse rate) and KLZ (lower zone recession constant). Other parameters of some relative significance were found to be CFX (degree days correction factor), BETA (soil moisture parameter) and FC (field capacity). This indicates that only seven of the 15 parameters played important roles in the fitting of models to observed discharge. This suggests either the possibility of using a smaller set of parameters for the PEST optimisations or developing an HBV-type model with a more parsimonious set of calibrated parameters. However, model calibration with respect to other objective functions or observational timeseries (for example, snow cover) may rely on the presence of other parameters not found to be sensitive in the model calibrations based solely on observed streamflow reported here.

9 References

Alfnes, E. 2007. Ekstremnedbør beregnet fra serier med gridbasert areanedbør. Met.no Report 1/2007, 22 p.

Alfnes, E., E. Langsholt, T. Skaugen. and H.-C. Udnæs, 2005. Updating snow reservoirs in hydrological models from satellite-observed snow covered areas. NVE Report No. 4 – 2005.

Bates, B.C., and E.P. Campbell. 2001. A Markov chain Monte Carlo scheme for parameter estimation and inference in conceptual rainfall-runoff modeling. *Water Resour. Res. 37*, 937-941, doi:10.1029/2000WR900363.

Beldring, S., Engeland, K., Roald, L. A., Sælthun, N. R., Voksø, A. 2003. Estimation of parameters in a distributed precipitation-runoff model for Norway. *Hydrology and Earth System Sciences 7*, 304-316.

Beldring, *et al*. 2006. Climate change impacts on hydrological processes in Norway, 2071-2100. *NVE Report no.* 5 – 2006, 24 p. and appendices.

Bergström, S. 1976. Development and application of a conceptual runoff model for Scandinavian catchments. SMHI Report RH07.

Colleuille, H., E. Holmqvist, S. Beldring and L. E. Haugen, 2008. Betydningen av grunnvanns- og markvannsforhold for tilsig og kraftsituasjonen. NVE Report No. 12 – 2008.

Doherty, J., 2004. PEST: Model Independent Parameter Estimation. Fifth edition of user manual. Watermark Numerical Computing, Brisbane, Australia.

Duan, Q., S. Sorooshian and V. Gupta. 1992. Effective and efficient global optimization for conceptual rainfall-runoff models. *Water Resour. Res. 28*, 1015-1031, doi:10.1029/91WR02985.

Gupta, H.V., Sorooshian, S., Hogue, T.S., Boyle, D.P., 2003. Advances in automatic calibration of watershed models. In Q. Duan, H. Gupta, S. Sorooshian, A. Rousseau and R. Turcotte (eds.), *Water Science and Application Series* 6, pp. 197-211.

Haario, H., M. Laine, A. Mira and E. Saksman. 2006. DRAM:Efficient adaptive MCMC. *Stat. Comput., 16*, 339-354, doi:10.1007/s11222-006-9438-0.

Holmqvist, E. and I. K. Engen. 2008. Utvalg av tilsigsserier til Samkjøringsmodellen. *NVE Rapport nr* 7- 2008*,* 51 p.

Jansson, A., O. E. Tveito, P. Pirinen and M. Scharling. 2007. NORDGRID – a preliminary investigation on the potential for creation of a joint Nordic gridded climate dataset. *Met.no Report no. 03/2007,* 48 p.

Killingveit, Å. and N. R. Sælthun. 1995. Hydrological models. In *Hydropower Development 7: Hydrology.* Trondheim: Norwegian Institute of Technology, pp. 99-128.

Lin, Z., and D. E. Radcliffe. 2005. Automatic calibration and predictive uncertainty analysis of a semidistributed watershed model. *Vadose Zone J.,5,* 248-260, doi:10.2136/vzj2004.0025.

Liu, Y.B., S. Gebremeskel, S., De Smedt., F., Hoffmann, L., and L. Pfister. 2006. Predicting storm runoff from different land-use classes using a geographical information system-based distributed model. *Hydrol. Process. 20,* 533-548, doi: 10.1002/hyp.5920.

Marquardt, D. 1963. An algorithm for Least-Squares Estimation of Nonlinear Parameters. *SIAM Journal on Applied Mathematics 11,*431-441, doi:10.1137/0111030.

Mohr, M. 2008. New routines for gridding of temperature and precipitation observations for "seNorge.no". *Met.no Note no. 08/2008.* 40 p.

Mohr, M. and O. E. Tveito. 2008. Daily temperature and precipitation maps with 1 km resolution derived from Norwegian weather observations. Abstracts from *AMS 17th Conference on Applied Climatology*, 11-15 August,Whistler, BC, Canada.

Petterson, L.E. 2004. Aktive vannføringsstasjoner i Norge. *NVE Rapport nr* 16 – 2004, 55 p.

Skahill, B.E. and J. Doherty. 2006. Efficient accommodation of local minima in watershed model calibration. *J. Hydrol. 329,*122-139, doi: 10.1016/j.jhydrol.2006.02.005.

Solomatine, D.P., Y.B. Dibike and N. Kukuric. 1999. Automatic calibration of groundwater models using global optimization techniques. *Hydrological Sciences – Jounal des Sciences Hydrologiques 44*, 879-894.

Sælthun, N.S. 1996. The Nordic HBV Model. *NVE Publication no*. 07, 26 pp.

Tveito, O.E., E. Førland, R. Heino, I. Hansen-Bauer, H. Alexandersson, B. Dahlström, A. Drebs, C. Kem-Hansen, T. Jónsson, E. Vaarby Laursen and Y. Westman. 2000. Nordic temperature maps. *DNMI KLIMA Report,* 09/00.

Tveito, O.E. and E.J. Førland 1999. Mapping temperatures in Norway applying terrain information, geostatistics and GIS. *Norsk Geogr. Tidsskr. 53,* 202-212.

Tveito, O.E., Bjørdal, I., Skjelvåg, A.O. and B. Aune. 2005.A GIS-based agro-ecological decision system based on gridded climatology, *Met. Apps. 12*, 57-68.

Vrugt, J.A., H.V. Gupta, W. Bouten, and S. Sorooshian (2003), A Shuffled Complex Evolution Metropolis algorithm for optimization and uncertainty assessment of hydrologic model parameters, *Water Resour. Res.39*, 1201 - 1215, doi:10.1029/2002WR001642.

Appendix 1 - Catchments for HBV model calibration

Station number	**Station name**	**Catchment area (km^2)**	**Available Q data** (deviations from standard period indicated in bold)	**Used in model for energy prognoses**
2.11	Narsjø	119	1961 - 2006	Yes
2.142	Knappom	1648	1961 - 2006	Yes
2.145	Losna	11208	1961 - 2006	No
2.265	Unsetåa	621	1961 - 2006	No
2.268	Akslen	795	1961 - 2006	Yes
2.279	Kråkfoss	433	**1966** - 2006	Yes
2.27	Aulestad	866	1961 - 2006	No
2.291	Tora	263	**1966** - 2006	Yes
2.32	Atnasjø	463	1961 - 2006	Yes
2.323	Fura	45	**1970** - 2006	Yes
2.604	Elverum	15449	1961 - 2006	No
2.614	Rosten	1828	1961 - 2006	Yes
2.634	Lena	181	**1991** - 2006	Yes
3.22	Høgfoss	299	**1976** - 2006	Yes
6.10	Gryta	7	**1967** - 2006	Yes
8.2	Bjørnegårdssvingen	190	**1968** - 2006	No
8.6	Sæternbekken	6	**1971** - 2006	No
12.171	Hølervatn	79	**1968** - 2006	Yes
12.178	Eggedal	309	**1972** - 2006	Yes
12.192	Sundbyfoss	74	**1976** - 2006	No
12.193	Fiskum	52	**1976** - 2006	Yes
12.215	Storeskar	120	**1987** - 2006	Yes
12.70	Etna	570	1961 - 2006	Yes
15.74	Skorge	60	1961 - 2006	No
15.79	Orsjoren	1177	**1982** - 2006	No
16.132	Gjuvå	33	**1981 - 2002**	Yes
16.140	Kvenna	822	**2001 - 2004**	No
16.193	Hørte	156	1961 - 2006	Yes
16.66	Groset	6	1961 - 2006	Yes
16.75	Tannsvatn	118	1961 - 2006	Yes
18.10	Gjerstad	238	**1980** - 2006	Yes
20.2	Austenå	276	1961 - 2006	Yes
21.47	Lislefjødd	19	**1974** - 2006	Yes
22.16	Myglevatn	182	1961 - 2006	Yes
22.22	Søgne	206	**1974 - 2005**	Yes
24.3	Møska	121	**1978** - 2006	No
24.9	Tingvatn	272	1961 - 2006	Yes
25.24	Gjuvvatn	97	**1971** - 2006	Yes
25.8	Mygland	47	1961 - 2006	No
26.20	Årdal	77	**1970** - 2006	Yes
26.26	Jogla	31	**1973** - 2006	Yes
27.16	Bjordal	124	**1987** - 2006	Yes
27.24	Helleland	186	1961 - 2006	No

Station number	Station name	Catchment area (km^2)	Available Q data (deviations from standard period indicated in bold)	Used in model for energy prognoses
27.26	Hetland	70	1961 - 2006	No
28.7	Haugland	140	1961 - 2006	Yes
35.16	Djupadalsvatn	45	**1990** - 2006	Yes
41.1	Stordalsvatn	129	1961 - 2006	Yes
42.2	Djupevad	31	**1963** - 2006	Yes
46.9	Fønnerdalsvatn	7	**1980** - 2006	Yes
48.1	Sandvenvatn	468	1961 - 2006	Yes
48.5	Reinsnosvatn	120	1961 - 2006	Yes
50.1	Hølen	232	1961 - 2006	Yes
50.13	Bjoreio	263	**1983** - 2006	Yes
55.4	Røykenes	50	1961 - 2006	Yes
55.5	Dyrdalsvatn	3	**1977** - 2006	No
62.10	Myrkdalsvatn	159	**1964** - 2006	Yes
62.18	Svartavatn	72	**1987** - 2006	Yes
62.5	Bulken	1094	1961 - 2006	Yes
72.5	Brekke bru	267	1961 - 2006	Yes
73.27	Sula	31	**1991** - 2006	Yes
75.23	Krokenelv	46	1961 - 2006	No
76.5	Nigardsbrevatn	65	**1962** - 2006	Yes
77.3	Sogndalsvatn	110	**1962** - 2006	Yes
78.8	Bøyumselv	40	**1965** - 2006	Yes
79.3	Nessedalselv	30	**1983** - 2006	Yes
82.4	Nautsundvatn	219	1961 - 2006	Yes
83.2	Viksvatn	507	1961 - 2006	Yes
84.11	Hovefoss	234	**1963** - 2006	Yes
86.12	Skjerdalselv	24	**1982** - 2006	Yes
87.3	Teita bru	219	**1970** - 2006	Yes
88.4	Lovatn	235	1961 - 2006	Yes
97.1	Fetvatn	89	1961 - 2006	Yes
98.4	Øye	139	1961 - 2006	Yes
103.1	Storhølen	437	**1971** - 2006	No
103.4	Horgheim	1099	**1971** - 2006	No
104.23	Vistdal	66	**1975** - 2006	No
105.1	Øren, Osenelv	138	1961 - 2006	No
107.3	Farstad	24	**1965** - 2006	No
109.42	Elverhøy bru	2442	**1975** - 2006	No
109.9	Risefoss	744	1961 - 2006	Yes
112.8	Rinna	91	**1969** - 2006	Yes
122.11	Eggafoss	653	1961 - 2006	Yes
122.9	Gaulfoss	3079	1961 - 2006	Yes
123.31	Kjelstad	142	1961 - 2006	Yes
124.2	Høggås bru	495	1961 - 2006	Yes
127.11	Veravatn	175	**1966** - 2006	Yes
127.13	Dillfoss	480	**1981** - 2006	No
133.7	Krinsvatn	207	1961 - 2006	Yes
138.1	Øyungen	239	1961 - 2006	Yes
139.15	Bjørnstad	1036	1961 - 2006	No

Station number	**Station name**	**Catchment area (km^2)**	**Available Q data** (deviations from standard period indicated in bold)	**Used in model for energy prognoses**
139.35	Trangen	854	1961 - 2006	Yes
148.2	Mevatn	109	**1973** - 2006	Yes
151.15	Nervoll	653	**1968** - 2006	Yes
152.4	Fustvatn	526	1961 - 2006	Yes
156.10	Berget	211	1961 - 2006	Yes
156.19	Bredek	229	**1967 - 2001**	No
157.3	Vassvatn	17	1961 - 2006	Yes
162.3	Skarsvatn	146	1961 - 2006	Yes
163.5	Junkerdalselv	419	1961 - 2006	Yes
165.6	Strandå	24	1961 - 2006	Yes
168.2	Mørsvik bru	31	**1985** - 2006	Yes
173.8	Coarveveij	64	**1972** - 2006	No
174.3	Øvstevatn	28	1961 - 2006	Yes
191.2	Øvrevatn	526	1961 - 2006	Yes
196.35	Malangsfoss	3237	1961 - 2006	No
200.4	Skogsfjordvatn	135	1961 - 2006	Yes
206.3	Manndalen bru	188	**1971** - 2006	Yes
208.3	Svartfossberget	1929	**1981** - 2006	No
212.10	Masi	5626	**1966** - 2006	Yes
212.49	Halsnes	145	1961 - 2006	No
223.2	Lombola	878	1961 - 2006	No
234.13	Vækkava	2078	**1973 - 2005**	No
234.18	Polmak	14157	1961 - 2006	Yes
241.1	Bergeby	248	1961 - **1996**	No
247.3	Karpelv	138	**1974 - 2001**	Yes
311.460	Engeren	395	1961 - 2006	Yes
311.6	Nybergsund	4420	1961 - 2006	No

Appendix 2 – Vegtype.dat file for land cover classes

Type	Number	ICMAX	CXREL	TSDIFF	CVSNOW	FCREL	LPDEL	EPVAR	SDALPHA	SDNU
Snaufjell (Rock)	1	0.0	1.0	0.0	0.3	0.2	1.0	0.1	0.007	0.0172
Skog (Forest)	2	2.0	0.9	0.0	0.3	1.0	0.6	1.0	0.0321	0.0786
Myr (Bog/Marsh)	3	0.1	1.1	0.0	0.3	2.5	0.7	0.8	0.0321	0.0786
Jbruk (Arable/Meadow)	4	0.1	1.1	0.1	0.3	0.4	0.8	1.0	0.0321	0.0786
Annet (Other)	5	0.0	1.0	0.0	0.5	0.5	0.8	1.0	0.0321	0.0786

Appendix 3 – Results of HBV calibration and validation by catchment

Station number	Station name	Catchment area (km^2)	Calibration period	Validation periods	N - S value Validation (Daily)	N - S value All years (Daily)	N - S value All years (Weekly)	Volumetric bias (%) All years
2.11	Narsjø	119	1981 - 2000	1961 - 1980; 2001 - 2006	0.80	0.83	0.87	-2.92
2.142	Knappom	1648	1981 - 2000	1961 - 1980; 2001 - 2006	0.78	0.81	0.85	-2.89
2.145	Losna	11208	1981 - 2000	1961 - 1980; 2001 - 2006	0.86	0.88	0.91	-2.09
2.265	Unsetåa	621	1981 - 2000	1961 - 1980; 2001 - 2006	0.70	0.74	0.76	-3.28
2.268	Akslen	795	1981 - 2000	1961 - 1980; 2001 - 2006	0.84	0.85	0.90	-4.67
2.279	Kråkfoss	433	1981 - 2000	1966 - 1980; 2001 - 2006	0.84	0.82	0.86	-0.80
2.27	Aulestad	866	1981 - 2000	1961 - 1980; 2001 - 2006	0.74	0.73	0.80	-3.49
2.291	Tora	263	1981 - 2000	1966 - 1980; 2001 - 2006	0.81	0.85	0.89	-6.22
2.32	Atnasjø	463	1981 - 2000	1961 - 1980; 2001 - 2006	0.81	0.84	0.89	-2.71
2.323	Fura	45	1981 - 2000	1970 - 1980; 2001 - 2006	0.6	0.62	0.78	-2.23
2.604	Elverum	15449	1981 - 2000	1961 - 1980; 2001 - 2006	0.87	0.88	0.90	-1.33
2.614	Rosten	1828	1981 - 2000	1961 - 1980; 2001 - 2006	0.86	0.89	0.93	-0.31
2.634	Lena	181	1991 - 2000	2001 - 2006	0.78	0.76	0.85	-3.13
3.22	Høgfoss	299	1981 - 2000	1976 - 1980; 2001 - 2006	0.81	0.76	0.84	-3.13
6.10	Gryta	7	1981 - 2000	1967 - 1980; 2001 - 2006	0.71	0.71	0.80	-2.78
8.2	Bjørnegårdssvingen	190	1981 - 2000	1968 - 1980; 2001 - 2006	0.74	0.71	0.81	3.26
8.6	Sæternbekken	6	1981 - 2000	1971 - 1980; 2001 - 2006	0.56	0.53	0.72	1.41
12.171	Hølervatn	79	1981 - 2000	1968 - 1980; 2001 - 2006	0.85	0.84	0.87	-2.08
12.178	Eggedal	309	1981 - 2000	1972 - 1980; 2001 - 2006	0.81	0.80	0.87	6.87
12.192	Sundbyfoss	74	1981 - 2000	1976 - 1980; 2001 - 2006	0.70	0.72	0.82	-4.69
12.193	Fiskum	52	1981 - 2000	1976 - 1980; 2001 - 2006	0.69	0.70	0.79	0.24
12.215	Storeskar	120	1987 - 2000	2001 - 2006	0.79	0.80	0.86	-1.20
12.70	Etna	570	1981 - 2000	1961 - 1980; 2001 - 2006	0.78	0.77	0.79	-0.34
15.74	Skorge	60	1981 - 2000	1961 - 1980; 2001 - 2006	0.80	0.75	0.85	-3.18

Station number	Station name	Catchment area (km^2)	Calibration period	Validation periods	N - S value Validation (Daily)	N - S value All years (Daily)	N - S value All years (Weekly)	Volumetric bias (%) All years
15.79	Orsjoren	1177	1988 - 2000	1982 - 1987; 2001 - 2006	0.79	0.83	0.85	1.40
16.132	Gjuvå	33	1981 - 2000	2000 - 2002	0.79	0.81	0.87	-1.81
16.140	Kvenna	822	2002 - 2003	2001 - 2004	0.69	0.75	0.78	-17.81
16.193	Hørte	156	1981 - 2000	1961 - 1980; 2001 - 2006	0.66	0.67	0.83	0.96
16.66	Groset	6	1981 - 2000	1961 - 1980; 2001 - 2006	0.64	0.70	0.75	-5.47
16.75	Tannsvatn	118	1981 - 2000	1961 - 1980; 2001 - 2006	0.78	0.81	0.83	0.66
18.10	Gjerstad	238	1981 - 2000	2000 - 2006	0.78	0.75	0.85	-0.25
20.2	Austenå	276	1981 - 2000	1961 - 1980; 2001 - 2006	0.73	0.76	0.81	-3.71
21.47	Lislefjødd	19	1983 - 1995	1974 - 1980	0.49	0.58	0.71	-1.33
22.16	Myglevatn	182	1981 - 2000	1961 - 1980; 2001 - 2006	0.76	0.78	0.83	-0.18
22.22	Søgne	206	1981 - 2000	1974 - 1980; 2001 - 2005	0.81	0.81	0.90	-2.11
24.3	Møska	121	1981 - 2000	1978 - 1980; 2001 - 2006	0.87	0.87	0.91	-1.27
24.9	Tingvatn	272	1981 - 2000	1961 - 1980; 2001 - 2006	0.88	0.89	0.92	-0.87
25.24	Gjuvvatn	97	1981 - 2000	1971 - 1980; 2001 - 2006	0.83	0.83	0.85	-2.09
25.8	Mygland	47	1981 - 2000	1961 - 1980; 2001 - 2006	0.60	0.63	0.81	0.56
26.20	Årdal	77	1981 - 2000	1970 - 1980; 2001 - 2006	0.71	0.77	0.86	2.51
26.26	Jogla	31	1981 - 2000	1973 - 1980; 2001 - 2006	0.63	0.66	0.82	1.29
27.16	Bjordal	124	1987 - 1996	1987 - 2006	0.69	0.68	0.81	-2.18
27.24	Helleland	186	1981 - 2000	1961 - 1980; 2001 - 2006	0.65	0.67	0.81	-4.79
27.26	Hetland	70	1981 - 2000	1961 - 1980; 2001 - 2006	0.72	0.73	0.86	-1.09
28.7	Haugland	140	1981 - 2000	1961 - 1980; 2001 - 2006	0.76	0.78	0.88	-4.82
35.16	Djupadalsvatn	45	1990 - 2000	2001 - 2006	0.79	0.78	0.83	-1.15
41.1	Stordalsvatn	129	1981 - 2000	1961 - 1980; 2001 - 2006	0.77	0.80	0.83	-0.25
42.2	Djupevad	31	1981 - 2000	1963 - 1980; 2001 - 2006	0.58	0.52	0.76	-2.75
46.9	Fønnerdalsvatn	7	1981 - 2000	2001 - 2006	0.69	0.68	0.81	-0.04
48.1	Sandvenvatn	468	1981 - 2000	1961 - 1980; 2001 - 2006	0.76	0.75	0.82	-2.74

Station number	Station name	Catchment area (km^2)	Calibration period	Validation periods	N - S value Validation (Daily)	N - S value All years (Daily)	N - S value All years (Weekly)	Volumetric bias (%) All years
48.5	Reinsnosvatn	120	1981 - 2000	1961 - 1980; 2001 - 2006	0.76	0.76	0.79	1.03
50.1	Hølen	232	1981 - 2000	1961 - 1980; 2001 - 2006	0.64	0.74	0.79	-2.96
50.13	Bjoreio	263	1983 - 1995	1996 - 2006	0.75	0.78	0.82	-0.14
55.4	Røykenes	50	1981 - 2000	1961 - 1980; 2001 - 2006	0.67	0.70	0.87	-2.16
55.5	Dyrdalsvatn	3	1983 - 1995	1977 - 1983; 2001 - 2006	0.48	0.53	0.72	4.02
62.10	Myrkdalsvatn	159	1981 - 2000	1964 - 1980; 2001 - 2006	0.75	0.75	0.83	0.08
62.18	Svartavatn	72	1987 - 2000	2001 - 2006	0.46	0.51	0.67	-0.51
62.5	Bulken	1094	1981 - 2000	1961 - 1980; 2001 - 2006	0.86	0.86	0.90	0.17
72.5	Brekke bru	267	1981 - 2000	1961 - 1980; 2001 - 2006	0.69	0.73	0.79	10.34
73.27	Sula	31	1991 - 2000	1967 -1980; 2001 - 2006	0.75	0.76	0.78	-6.89
75.23	Krokenelv	46	1970 - 1991	1992 - 2006	0.61	0.57	0.71	2.33
76.5	Nigardsbrevatn	65	1981 - 2000	1962 - 1980; 2001 - 2006	0.93	0.92	0.95	0.19
77.3	Sogndalsvatn	110	1981 - 2000	1962 - 1980; 2001 - 2006	0.67	0.67	0.80	1.56
78.8	Bøyumselv	40	1981 - 2000	1965 - 1980; 2001 - 2006	0.72	0.73	0.82	-9.07
79.3	Nessedalselv	30	1983 - 2000	2001 - 2006	0.49	0.60	0.74	1.97
82.4	Nautsundvatn	219	1981 - 2000	1961 - 1980; 2001 - 2006	0.74	0.75	0.85	7.71
83.2	Viksvatn	507	1981 - 2000	1961 - 1980; 2001 - 2006	0.86	0.88	0.88	1.69
84.11	Hovefoss	234	1981 - 2000	1963 - 1980; 2001 - 2006	0.55	0.56	0.73	-5.56
86.12	Skjerdalselv	24	1982 - 2000	2001 - 2006	0.47	0.53	0.65	-1.95
87.3	Teita bru	219	1981 - 2000	1970 - 1980; 2001 - 2006	0.65	0.65	0.84	-2.94
88.4	Lovatn	235	1981 - 2000	1961 - 1980; 2001 - 2006	0.90	0.90	0.92	2.71
97.1	Fetvatn	89	1981 - 2000	1961 - 1980; 2001 - 2006	0.51	0.54	0.71	-0.13
98.4	Øye	139	1981 - 2000	1961 - 1980; 2001 - 2006	0.64	0.66	0.78	1.08
103.1	Storhølen	437	1981 - 2000	1971 - 1980; 2001 - 2006	0.87	0.87	0.92	-2.30
103.4	Horgheim	1099	1981 - 2000	1971 - 1980; 2001 - 2006	0.88	0.89	0.92	-0.97
104.23	Vistdal	66	1981 - 2000	1975 - 1980; 2001 - 2006	0.60	0.59	0.77	-0.78

Station number	Station name	Catchment area (km^2)	Calibration period	Validation periods	N - S value Validation (Daily)	N - S value All years (Daily)	N - S value All years (Weekly)	Volumetric bias (%) All years
105.1	Øren, Osenelv	138	1981 - 2000	1961 - 1980; 2001 - 2006	0.64	0.68	0.75	1.22
107.3	Farstad	24	1981 - 2000	1965 - 1980; 2001 - 2006	0.65	0.68	0.79	0.55
109.42	Elverhøy bru	2442	1981 - 2000	1975 - 1980; 2001 - 2006	0.83	0.85	0.90	8.28
109.9	Risefoss	744	1981 - 2000	1961 - 1980; 2001 - 2006	0.73	0.80	0.90	0.41
112.8	Rinna	91.1	1981 - 2000	1969 - 1980; 2001 - 2006	0.71	0.71	0.83	-0.80
122.11	Eggafoss	653	1981 - 2000	1961 - 1980; 2001 - 2006	0.87	0.88	0.93	1.15
122.9	Gaulfoss	3079	1981 - 2000	1961 - 1980; 2001 - 2006	0.81	0.83	0.90	-0.71
123.31	Kjelstad	142	1981 - 2000	1961 - 1980; 2001 - 2006	0.55	0.63	0.76	4.48
124.2	Høggås bru	495	1981 - 2000	1961 - 1980; 2001 - 2006	0.77	0.78	0.87	1.70
127.11	Veravatn	175	1981 - 2000	1966 - 1980; 2001 - 2006	0.84	0.86	0.89	2.46
127.13	Dillfoss	480	1981 - 2000	2001 - 2006	0.69	0.73	0.85	3.56
133.7	Krinsvatn	207	1981 - 2000	1961 - 1980; 2001 - 2006	0.75	0.77	0.82	-3.29
138.1	Øyungen	239	1981 - 2000	1961 - 1980; 2001 - 2006	0.70	0.75	0.80	-0.13
139.15	Bjørnstad	1036	1981 - 2000	1961 - 1980; 2001 - 2006	0.50	0.56	0.60	-1.85
139.35	Trangen	854	1981 - 2000	1961 - 1980; 2001 - 2006	0.69	0.73	0.80	2.06
148.2	Mevatn	109	1981 - 2000	1973 - 1980; 2001 - 2006	0.78	0.76	0.78	4.14
151.15	Nervoll	653	1981 - 2000	1968 - 1980; 2001 - 2006	0.86	0.87	0.91	-0.11
152.4	Fustvatn	526	1981 - 2000	1961 - 1980; 2001 - 2006	0.82	0.80	0.82	-2.63
156.10	Berget	211	1981 - 2000	1961 - 1980; 2001 - 2006	0.82	0.83	0.90	1.53
156.19	Bredek	229	1981 - 2000	1967 - 1980; 2001	0.77	0.76	0.86	-0.04
157.3	Vassvatn	16.6	1980 - 1997	1961 - 1980; 2001 - 2006	0.72	0.72	0.84	-3.30
162.3	Skarsvatn	146	1981 - 2000	1961 - 1980; 2001 - 2006	0.57	0.60	0.63	4.92
163.5	Junkerdalselv	419	1981 - 2000	1961 - 1980; 2001 - 2006	0.68	0.75	0.86	3.65
165.6	Strandå	23.9	1981 - 2000	1961 - 1980; 2001 - 2006	0.70	0.72	0.80	2.83
168.2	Mørsvik bru	31.3	1985 - 2000	2001 - 2006	0.78	0.80	0.86	-0.48
173.8	Coarveveij	63.6	1981 - 2000	1972 - 1980; 2001 - 2006	0.89	0.88	0.90	-0.96

Station number	Station name	Catchment area (km^2)	Calibration period	Validation periods	N - S value Validation (Daily)	N - S value All years (Daily)	N - S value All years (Weekly)	Volumetric bias (%) All years
174.3	Øvstevatn	28.4	1981 - 2000	1961 - 1980; 2001 - 2006	0.71	0.75	0.82	-3.12
191.2	Øvrevatn	526	1981 - 2000	1961 - 1980; 2001 - 2006	0.87	0.86	0.90	-0.74
196.35	Malangsfoss	3237	1981 - 2000	1961 - 1980; 2001 - 2006	0.66	0.75	0.77	-1.79
200.4	Skogsfjordvatn	135	1981 - 2000	1961 - 1980; 2001 - 2006	0.68	0.71	0.74	8.04
206.3	Manndalen bru	188	1981 - 2000	1971 - 1980; 2001 - 2006	0.82	0.85	0.90	3.94
208.3	Svartfossberget	1929	1981 - 2000	2001 - 2006	0.70	0.82	0.86	6.13
212.10	Masi	5626	1981 - 2000	1966 - 1980; 2001 - 2006	0.85	0.85	0.87	-4.24
212.49	Halsnes	145	1981 - 2000	1961 - 1980; 2001 - 2006	0.84	0.86	0.90	0.29
223.2	Lombola	878	1981 - 2000	1961 - 1980; 2001 - 2006	0.81	0.86	0.89	2.47
234.13	Vækkava	2078	1981 - 2000	1973 - 1980; 2001 - 2005	0.81	0.87	0.88	-1.50
234.18	Polmak	14157	1981 - 2000	1961 - 1980; 2001 - 2006	0.85	0.85	0.89	0.36
241.1	Bergeby	248	1981 - 1996	1961 - 1980	0.70	0.69	0.72	3.08
247.3	Karpelv	138	1983 - 1995	1974 - 1982; 2001	0.86	0.83	0.87	3.09
311.460	Engeren	395	1981 - 2000	1961 - 1980; 2001 - 2006	0.86	0.88	0.90	-6.80
311.6	Nybergsund	4420	1981 - 2000	1961 - 1980; 2001 - 2006	0.88	0.89	0.90	-5.18

Appendix 4 – PEST control file

```
pcf
* control data
restart estimation
15 6941 9 0 2
1 2 single point 1 0 0
5.0 2.0 0.3 0.03 10
3.0 3.0 0.001
0.1
30 0.01 3 3 0.01 3
1 1 1
* parameter groups
tres relative  0.03   0.01  always_2  2 parabolic
cx   relative  0.0125 0.05  always_2  2 parabolic
kor  relative  0.025  0.025 always_2  2 parabolic
tgrd relative  0.02   0.001 always_2  2 parabolic
pgrd relative  0.02   0.001 always_2  2 parabolic
kuz2 relative  0.03   0.01  always_2  2 parabolic
uz1  relative  0.025  1.0   always_2  2 parabolic
kuz1 relative  0.05   0.005 always_2  2 parabolic
klz  relative  0.02   0.001 always_2  2 parabolic
* parameter data
tx   none  relative    1.0   -1.0      2.0    tres  1.0   0.0 1
ts   none  relative    0.0   -1.0      2.0    tres  1.0   0.0 1
cx    log  factor      3.7    1.0      5.0    cx    1.0   0.0 1
pkor  log  factor      1.4    0.8      3.0    kor   1.0   0.0 1
skor  log  factor      1.2    1.0      3.0    kor   1.0   0.0 1
ttgd none  factor     -0.7   -1.0     -0.5    tgrd  1.0   0.0 1
tvgd none  factor     -0.5   -0.7     -0.3    tgrd  1.0   0.0 1
pgrd none  relative    0.02   0.0      0.1    pgrd  1.0   0.0 1
fc    log  factor    150.0   50.0    500.0    uz1   1.0   0.0 1
beta  log  factor      3.0    1.0      4.0    kor   1.0   0.0 1
kuz2 none  factor      0.5    0.1      1.0    kuz2  1.0   0.0 1
uz1   log  factor     40.0   10.0    100.0    uz1   1.0   0.0 1
kuz1 none  factor      0.15   0.01     1.0    kuz1  1.0   0.0 1
perc  log  factor      1.2    0.5      2.0    kor   1.0   0.0 1
klz  none  factor      0.02   0.001    0.1    klz   1.0   0.0 1
* observation groups
sim
diff
* observation data
accd     0.0    0.5   sim
* model command line
./run1.pl
* model input/output
param.tpl param.dat
qsim.ins PRTFIL.RES
res.ins PRTFIL.RES
```

This series is published by Norwegian Water Resources and Energy Directorate (NVE)

Published in the Report series 2009